

Performance Analysis of Source Image Estimators in Blind Source Separation

Zbyněk Koldovský and Francesco Nesta

¹Faculty of Mechatronics, Informatics, and Interdisciplinary Studies, Technical University of Liberec,

Studentská 2, 461 17 Liberec, Czech Republic. E-mail: zbynek.koldovsky@tul.cz,

fax:+420-485-353112, tel:+420-485-353534

²Conexant System, 1901 Main Street, Irvine, CA (USA). E-mail: francesco.nesta@conexant.com

Abstract

Blind methods often separate or identify signals or signal subspaces up to an unknown scaling factor. Sometimes it is necessary to cope with the scaling ambiguity, which can be done through reconstructing signals as they are received by sensors, because scales of the sensor responses (images) have known physical interpretations. In this paper, we analyze two approaches that are widely used for computing the sensor responses, especially, in Frequency-Domain Independent Component Analysis. One approach is the least-squares projection, while the other one assumes a regular mixing matrix and computes its inverse. Both estimators are invariant to the unknown scaling. Although frequently used, their differences were not studied yet. A goal of this work is to fill this gap. The estimators are compared through a theoretical study, perturbation analysis and simulations. We point to the fact that the estimators are equivalent when the separated signal subspaces are orthogonal, and vice versa. Two applications are shown, one of which demonstrates a case where the estimators yield substantially different results.

Index Terms

Beamforming, Blind Source Separation, Independent Component Analysis, Principal Component Analysis, Independent Vector Analysis

I. INTRODUCTION

The linear instantaneous complex-valued mixture model

$$\mathbf{x} = \mathbf{H}\mathbf{s} \quad \text{or} \quad \mathbf{X} = \mathbf{H}\mathbf{S} \quad (1)$$

describes many situations where multichannel signals are observed, especially those considered in the field of array processing [1] and Blind Source Separation (BSS) [2], [3]. The former equation is a vector-symbolic description of the model while the latter equation describes a batch of data.

The vector $\mathbf{x} = [x_1, \dots, x_d]^T$ represents d observed signals on sensors, $\mathbf{s} = [s_1, \dots, s_r]^T$ represents original signals, and \mathbf{H} is a $d \times r$ complex-valued mixing matrix representing the linear mixing system. Upper-case

bold letters such as \mathbf{X} and \mathbf{S} will denote matrices whose columns contain concrete samples of the respective signals; let the number of columns (samples) be N where $N \gg d$. We will focus on the regular case when the number of the observed signals d is the same as that of the original signals r , but later in the article we will also address an undetermined case where $r > d$. From this point forward, let \mathbf{H} be a $d \times d$ full rank matrix.

Consider a situation where only a subset of the original signals is of primary interest (e.g., only one particular source or the subspace spanned by some sources, so-called multidimensional source). Without a loss of generality, let \mathbf{s} be divided into two components $[\mathbf{s}_1; \mathbf{s}_2]$ where the sub-vectors \mathbf{s}_1 and \mathbf{s}_2 have, respectively, length m and $d - m$, $1 \leq m < d$. The former component will be referred to as *target component*, and the latter as *interference*. Correspondingly, let \mathbf{H} be divided as $[\mathbf{H}_1 \mathbf{H}_2]$ where the sub-matrices \mathbf{H}_1 and \mathbf{H}_2 have dimensions $d \times m$ and $d \times (d - m)$, respectively. Then (1) can be written as

$$\mathbf{x} = \mathbf{H}_1 \mathbf{s}_1 + \mathbf{H}_2 \mathbf{s}_2. \quad (2)$$

The terms $\mathbf{H}_1 \mathbf{s}_1$ and $\mathbf{H}_2 \mathbf{s}_2$ correspond to the contributions of \mathbf{s}_1 and \mathbf{s}_2 , respectively, for the mixture \mathbf{x} , and will be denoted as $\mathbf{s}^i \triangleq \mathbf{H}_i \mathbf{s}_i$, $i \in \{1, 2\}$. If, for example, \mathbf{s}_2 is not active, then $\mathbf{x} = \mathbf{s}^1$, which is equal to the observations of \mathbf{s}_1 on the sensors, that is, the *sensor response* or *source image* of \mathbf{s}_1 .

In audio applications, \mathbf{s}_1 is often a scalar signal ($m = 1$) representing a point source located in the room, and the model (1) describes linear mixing in the frequency domain for a particular frequency bin [4], [5], [6], [7]. For $m > 1$, \mathbf{s}_1 can correspond to a subgroup of speakers [8]. In biomedical applications, \mathbf{s}_1 or \mathbf{s}_2 can consist of components related to a target activity such as muscular artifacts in electroencephalogram (EEG) [9], maternal or fetal electrocardiogram (ECG) [10], and so forth.

The problem of retrieving \mathbf{s}^i from \mathbf{x} is often solved with the aid of methods for Blind Source Separation. The objective of BSS is to separate the original signals based purely on their general properties (e.g., independence, sparsity or nonnegativity). In a general sense, BSS involves Principal Component Analysis (PCA), Independent Component Analysis (ICA) [2], [11], Independent Vector Analysis (IVA) [12], [13], Nonnegative Matrix Factorization [14], etc. Some methods separate all of the one-dimensional components of \mathbf{s} [15], [16], extract selected components only [17], or separate multidimensional components; see, e.g., [18], [19], [20], [21], [22]. The separation can also proceed in two steps where a steering vector/matrix (e.g., \mathbf{H}_1) is identified first, while the signals are separated in the second step using an array processor such as the minimum variance distortion-less (MVDR) beamformer [23].

The blind separation or identification is often not unique. For example, the order and scaling factors of the separated components are random and cannot be determined without additional assumptions. Throughout this paper, we will always assume that the problem of the random order (known as the permutation problem) has already been resolved, so the subspaces in (2) are correctly identified; for practical methods solving the permutation problem, see, e.g., [5], [24], [25].

The reconstruction of the signal images is a way to cope with the scaling ambiguity [7]. The advantage is that \mathbf{s}^i can be retrieved without prior knowledge of the scale of \mathbf{s}_i in (1) or in (2). The scale of \mathbf{s}^i has clear physical interpretation (e.g., voltage), so the retrieval is highly practical. For example, in the Frequency Domain ICA for audio source separation, the scaling ambiguity must be resolved within each frequency bin,

which is important for reconstructing the spectra of the separated signals in the time domain [5]. Some recent BSS methods aim to consider the observed signals directly as the sum of images of original sources, by which the scaling ambiguity is implicitly avoided and the number of unknown free parameters in the BSS model is decreased [4], [26], [27]. This motivates us for this study, because the way to reconstruct the signal images (either s^1 or s^2) is an important topic.

In this paper, we study two widely used methods to estimate the source images: One approach performs the least-squares projection of a separated source on the subspace spanned by \mathbf{X} . The other approach assumes that a blind estimate of a demixing transform is available and exploits its inverse to compute the sources' images. Both estimators are invariant to the unknown scaling of the separated sources. The goal of this study is to compare the estimators, which was not performed yet, and to provide a guidance which estimator is advantageous compared to the other from different aspects. We also show conditions under which the estimators are equivalent.

The following section introduces the estimators and points to their important properties and relations. Section III contains a perturbation analysis that studies cases where the estimated demixing transform contains "small" errors. Section IV studies properties of the least-squares estimator in underdetermined situations, that is, when there are more original signals than the observed ones. Section V presents results of simulations, and, finally, Section VI demonstrates two applications.

II. SOURCE IMAGE ESTIMATORS

Consider an exact demixing transform as a regular $d \times d$ matrix \mathbf{W} defined as such that

$$\mathbf{W}\mathbf{H} = \text{bdiag}(\mathbf{\Lambda}_1, \mathbf{\Lambda}_2), \quad (3)$$

where $\mathbf{\Lambda}_1$ and $\mathbf{\Lambda}_2$ are arbitrary nonsingular matrices representing the random scaling factors of dimensions $m \times m$ and $(d - m) \times (d - m)$, respectively; $\text{bdiag}(\cdot)$ denotes a block-diagonal matrix with the arguments on its block-diagonal. By applying \mathbf{W} to \mathbf{x} , the outputs are

$$\mathbf{y} = \mathbf{W}\mathbf{x} = \mathbf{W}\mathbf{H}\mathbf{s} = \begin{pmatrix} \mathbf{\Lambda}_1\mathbf{s}_1 \\ \mathbf{\Lambda}_2\mathbf{s}_2 \end{pmatrix} = \begin{pmatrix} \mathbf{y}_1 \\ \mathbf{y}_2 \end{pmatrix}. \quad (4)$$

The components $\mathbf{y}_1 = \mathbf{\Lambda}_1\mathbf{s}_1$ and $\mathbf{y}_2 = \mathbf{\Lambda}_2\mathbf{s}_2$ are separated in the sense that each is a mixture only of \mathbf{s}_1 and \mathbf{s}_2 , respectively.

Let \mathbf{W}_1 and \mathbf{W}_2 be sub-matrices of \mathbf{W} such that $\mathbf{W} = [\mathbf{W}_1; \mathbf{W}_2]$, and \mathbf{W}_1 contains the first m rows of \mathbf{W} , i.e., $\mathbf{y}_1 = \mathbf{W}_1\mathbf{x}$. From (3) it follows that \mathbf{W} is demixing if and only if¹ $\mathbf{W}_1\mathbf{H}_2 = \mathbf{0}$ and $\mathbf{W}_2\mathbf{H}_1 = \mathbf{0}$.

Throughout the paper we will occasionally use the following assumptions. Consider an estimated demixing matrix $\widehat{\mathbf{W}}$.

A1(i) The assumption that $\widehat{\mathbf{W}}_i\mathbf{H}_j = \mathbf{0}$ where $j \in \{1, 2\}, j \neq i$. Assuming an exact demixing transform thus corresponds to A1(1) simultaneously with A1(2).

A2 The assumption of *uncorrelatedness* of \mathbf{s}_1 and \mathbf{s}_2 means that $\text{E}[\mathbf{s}_1\mathbf{s}_2^H] = \mathbf{0}$.

¹A more general definition is that \mathbf{W} is demixing if and only if $\mathbf{W}_1\mathbf{H}_2\mathbf{s}_2 = \mathbf{0}$ and $\mathbf{W}_2\mathbf{H}_1\mathbf{s}_1 = \mathbf{0}$. However, we will assume that the mixing model (1) is determined, so cases where $\mathbf{W}_1\mathbf{H}_2\mathbf{s}_2 = \mathbf{0}$ while $\mathbf{W}_1\mathbf{H}_2 \neq \mathbf{0}$ and similar do not exist.

A3 The assumption of *orthogonality of \mathbf{Y}_1 and \mathbf{Y}_2* , that is,

$$\mathbf{Y}_1 \mathbf{Y}_2^H / N = \mathbf{0}, \quad (5)$$

in BSS also known as the orthogonal constraint [28], means that the sample-based estimate of $E[\mathbf{y}_1 \mathbf{y}_2^H]$ is exactly equal to zero.

In the determined case $r = d$ and under **A1(1)** and **A1(2)**, the condition (5) corresponds with

$$\mathbf{S}_1 \mathbf{S}_2^H / N = \mathbf{0}, \quad (6)$$

but not generally so when $r > d$. The latter condition could be seen as a stronger alternative to **A2**.

For example, the orthogonal constraint **A3** is used by some ICA methods such as is Symmetric or Deflation FastICA [15]. There are several reasons for this. First, **A2** is the necessary condition of independence of the original signals, so **A3** is a practical way to decrease the number of unknown parameters in ICA. Second, **A3** helps to achieve the global convergence (to find all independent components) and prevents algorithms from finding the same component twice. Finally, in the model (2) with the **A3** constraint, $\widehat{\mathbf{W}}_i$ is already determined up to a scaling matrix when $\widehat{\mathbf{W}}_j$ is given, $j \neq i$, and vice versa.

A. Reconstruction Using Inverse of Demixing Matrix

The estimator to retrieve \mathbf{s}^i described here will be abbreviated as INV.

Definition 1 (INV): Let $\widehat{\mathbf{W}} = [\widehat{\mathbf{W}}_1; \widehat{\mathbf{W}}_2]$ denote an estimated demixing matrix by a BSS method, and let $\widehat{\mathbf{A}}$ be its inverse matrix, i.e., $\widehat{\mathbf{A}} \triangleq \widehat{\mathbf{W}}^{-1}$. Let $\widehat{\mathbf{A}} = [\widehat{\mathbf{A}}_1 \widehat{\mathbf{A}}_2]$ be divided in the same way as the system matrix \mathbf{H} . Then, the INV estimator is defined as

$$\widehat{\mathbf{s}}_{\text{INV}}^i = \widehat{\mathbf{A}}_i \widehat{\mathbf{W}}_i \mathbf{x} \quad \text{or} \quad \widehat{\mathbf{S}}_{\text{INV}}^i = \widehat{\mathbf{A}}_i \widehat{\mathbf{W}}_i \mathbf{X}, \quad (7)$$

for $i \in \{1, 2\}$.

In particular, INV is popular in the frequency-domain ICA for audio source separation; see, e.g., [7], [6], [33]. The following two propositions point to its important properties.

Proposition 1 (consistency of INV): Consider an exact demixing transform \mathbf{W} satisfying **A1(1)** and **A1(2)**, that is, satisfying (3); let $\mathbf{A} = [\mathbf{A}_1 \mathbf{A}_2]$ be its inverse matrix. For $i \in \{1, 2\}$, it holds that

$$\widehat{\mathbf{s}}_{\text{INV}}^i = \mathbf{A}_i \mathbf{W}_i \mathbf{x} = \mathbf{s}^i. \quad (8)$$

Proof: By (3) it holds that $\mathbf{A}_i = \mathbf{H}_i \mathbf{\Lambda}_i^{-1}$. Then,

$$\mathbf{A}_i \mathbf{W}_i \mathbf{x} = \mathbf{A}_i \mathbf{W}_i (\mathbf{H}_1 \mathbf{s}_1 + \mathbf{H}_2 \mathbf{s}_2) \quad (9)$$

$$= \mathbf{A}_i \mathbf{W}_i \mathbf{H}_i \mathbf{s}_i \quad (10)$$

$$= \mathbf{H}_i \mathbf{\Lambda}_i^{-1} \mathbf{\Lambda}_i \mathbf{s}_i = \mathbf{H}_i \mathbf{s}_i = \mathbf{s}^i. \quad (11)$$

■

Proposition 2 (scaling invariance of INV): Let $\widehat{\mathbf{W}}$ be an estimated demixing transform and $\widehat{\mathbf{A}} = \widehat{\mathbf{W}}^{-1}$. The INV estimator is invariant to substitution $\widehat{\mathbf{W}} \leftarrow \text{bdiag}(\mathbf{\Lambda}_1, \mathbf{\Lambda}_2) \widehat{\mathbf{W}}$, where $\mathbf{\Lambda}_1$ and $\mathbf{\Lambda}_2$ are arbitrary nonsingular matrices of dimensions $m \times m$ and $(d - m) \times (d - m)$, respectively.

Proof: The proof follows from the fact that $[\mathbf{\Lambda}_1 \widehat{\mathbf{W}}_1; \mathbf{\Lambda}_2 \widehat{\mathbf{W}}_2]^{-1} = [\widehat{\mathbf{A}}_1 \mathbf{\Lambda}_1^{-1} \widehat{\mathbf{A}}_2 \mathbf{\Lambda}_2^{-1}]$. ■

One advantage is that the transform $\mathbf{A}_i \mathbf{W}_i$ is purely a function of \mathbf{W} and does not explicitly depend on the signals or on their statistics, e.g., on the sample-based covariance matrix. This makes the approach suitable for real-time processing [29].

On the other hand, $\mathbf{A}_i \mathbf{W}_i$ is a function of the whole \mathbf{W} through the matrix inverse; it does not depend solely on \mathbf{W}_i , as one would expect when only \mathbf{s}^i should be estimated. Formula (7) can thus be used only if the whole demixing \mathbf{W} is available. BSS methods extracting only selected components (e.g., one-unit FastICA [15]) cannot be applied together with (7). Next, it follows that potential errors in the estimate of \mathbf{W}_2 can have an adverse effect on the estimation of \mathbf{s}^1 . This is analyzed in Section III.

B. Least-squares reconstruction

Another approach to estimate \mathbf{s}^i is to find an optimum projection of the separated components back to the observed signals \mathbf{x} in order to find their contribution to them. A straightforward way is to use the quadratic criterion, that is, least squares, which gives two estimators that will be abbreviated by LS.

Definition 2 (LS): Let $\widehat{\mathbf{W}}_i$ denote an estimated part of a demixing matrix, $i \in \{1, 2\}$, $\mathbf{y}_i = \widehat{\mathbf{W}}_i \mathbf{x}$ and $\mathbf{Y}_i = \widehat{\mathbf{W}}_i \mathbf{X}$. The theoretical LS estimator of \mathbf{s}^i is defined as

$$\widehat{\mathbf{s}}_{\text{LS}}^i = \left(\arg \min_{\mathbf{v}} E [\|\mathbf{x} - \mathbf{V} \mathbf{y}_i\|^2] \right) \mathbf{x} \quad (12)$$

$$= \mathbf{C} \widehat{\mathbf{W}}_i^H (\widehat{\mathbf{W}}_i \mathbf{C} \widehat{\mathbf{W}}_i^H)^{-1} \widehat{\mathbf{W}}_i \mathbf{x}, \quad (13)$$

where $\mathbf{C} = E[\mathbf{x} \mathbf{x}^H]$. The practical LS estimator of \mathbf{S}^i is defined as

$$\widehat{\mathbf{S}}_{\text{LS}}^i = \left(\arg \min_{\mathbf{V}} \|\mathbf{X} - \mathbf{V} \mathbf{Y}_i\|_F^2 \right) \mathbf{X} \quad (14)$$

$$= \widehat{\mathbf{C}} \widehat{\mathbf{W}}_i^H (\widehat{\mathbf{W}}_i \widehat{\mathbf{C}} \widehat{\mathbf{W}}_i^H)^{-1} \widehat{\mathbf{W}}_i \mathbf{X}, \quad (15)$$

where $\widehat{\mathbf{C}} = \mathbf{X} \mathbf{X}^H / N$, and $\|\cdot\|_F$ denotes the Frobenius norm.

Proposition 3 (scaling invariance of LS): The estimators (12) and (14) are invariant to a scaling transform $\widehat{\mathbf{W}}_i \leftarrow \mathbf{\Lambda}_i \widehat{\mathbf{W}}_i$ where $\mathbf{\Lambda}_i$ is a nonsingular square matrix.

The proof of Proposition 3 is straightforward. It is worth pointing out that the LS estimators are purely functions of $\widehat{\mathbf{W}}_i$ as compared to INV. Also, they involve the covariance matrix or its sample-based estimate. However, their consistency is not guaranteed under A1(i) even if the assumption holds for both $i = 1, 2$ as assumed in Proposition 1. In fact, additional assumptions are needed as is shown by the following proposition.

Proposition 4: Let \mathbf{W}_i be a part of an exact demixing matrix, so A1(i) holds. Let $\mathbf{W}_i \mathbf{H}_i = \mathbf{\Lambda}_i$ be nonsingular. Then, under A2 it holds that

$$\widehat{\mathbf{s}}_{\text{LS}}^i = \mathbf{C} \mathbf{W}_i^H (\mathbf{W}_i \mathbf{C} \mathbf{W}_i^H)^{-1} \mathbf{W}_i \mathbf{x} = \mathbf{s}^i, \quad (16)$$

and under A3 it holds that

$$\widehat{\mathbf{S}}_{\text{LS}}^i = \widehat{\mathbf{C}} \widehat{\mathbf{W}}_i^H (\widehat{\mathbf{W}}_i \widehat{\mathbf{C}} \widehat{\mathbf{W}}_i^H)^{-1} \widehat{\mathbf{W}}_i \mathbf{X} = \mathbf{S}^i. \quad (17)$$

Proof: The proof will be given for (16) while the one for (17) is analogous.

According to (1) it holds that $\mathbf{C} = \mathbb{E}[\mathbf{x}\mathbf{x}^H] = \mathbf{H}\mathbf{C}_s\mathbf{H}^H$ where $\mathbf{C}_s = \mathbb{E}[\mathbf{s}\mathbf{s}^H]$. Under A2 it follows that \mathbf{C}_s has the block-diagonal structure $\mathbf{C}_s = \text{bdiag}(\mathbf{C}_{s_1}, \mathbf{C}_{s_2})$ where $\mathbf{C}_{s_1} \triangleq \mathbb{E}[\mathbf{s}_1\mathbf{s}_1^H]$ and $\mathbf{C}_{s_2} \triangleq \mathbb{E}[\mathbf{s}_2\mathbf{s}_2^H]$ are regular (because \mathbf{C}_s is assumed to be regular). Without a loss of generality, let $i = 1$. Since $\mathbf{W}_1\mathbf{H} = (\mathbf{\Lambda}_1 \mathbf{0})$,

$$\widehat{\mathbf{s}}_{\text{LS}}^i = \mathbf{C}\mathbf{W}_1^H(\mathbf{W}_1\mathbf{C}\mathbf{W}_1^H)^{-1}\mathbf{W}_1\mathbf{x} \quad (18)$$

$$= \mathbf{H}\mathbf{C}_s\mathbf{H}^H\mathbf{W}_1^H(\mathbf{W}_1\mathbf{H}\mathbf{C}_s\mathbf{H}^H\mathbf{W}_1^H)^{-1}\mathbf{W}_1\mathbf{H}\mathbf{s} \quad (19)$$

$$= \mathbf{H}_1\mathbf{C}_{s_1}\mathbf{\Lambda}_1^H(\mathbf{\Lambda}_1\mathbf{C}_{s_1}\mathbf{\Lambda}_1^H)^{-1}\mathbf{\Lambda}_1\mathbf{s}_1 \quad (20)$$

$$= \mathbf{H}_1\mathbf{s}_1 = \mathbf{s}^1. \quad (21)$$

■

It is worth pointing out that LS involves a matrix inverse, namely, of $\mathbf{W}_i\mathbf{C}\mathbf{W}_i^H$ or of $\mathbf{W}_i\widehat{\mathbf{C}}\mathbf{W}_i^H$. This matrix (actually, the (sample) covariance of $(\mathbf{Y}_i) \mathbf{y}_i$) has a lower dimension than \mathbf{W} and is more likely well conditioned so that the computation of its inverse is numerically stable.

C. On the equivalence between INV and LS under the orthogonal constraint

Without a loss of generality, assume that $\widehat{\mathbf{W}}_1$ is given. Under the assumption A3, $\widehat{\mathbf{W}}_2$ is already determined up to a scaling matrix through (5), so the whole $\widehat{\mathbf{W}}$ is actually available, and the INV estimator (7) can be applied. The goal here is to verify that, in this case, INV coincides with LS.

Let \mathbf{B} denote the unknown lower part of the entire demixing $\widehat{\mathbf{W}} = [\widehat{\mathbf{W}}_1; \mathbf{B}]$. Then,

$$\widehat{\mathbf{W}}\mathbf{X} = \begin{pmatrix} \widehat{\mathbf{W}}_1\mathbf{X} \\ \mathbf{B}\mathbf{X} \end{pmatrix} = \begin{pmatrix} \mathbf{Y}_1 \\ \mathbf{Y}_2 \end{pmatrix}. \quad (22)$$

The condition (5) requires that

$$\mathbf{B}\widehat{\mathbf{C}}\widehat{\mathbf{W}}_1^H = \mathbf{0}, \quad (23)$$

which means that the rows of \mathbf{B} are orthogonal to the columns of $\widehat{\mathbf{C}}\widehat{\mathbf{W}}_1^H$. It can be verified that any \mathbf{B} of the form

$$\mathbf{B} = \mathbf{Q}(\mathbf{I} - \widehat{\mathbf{C}}\widehat{\mathbf{W}}_1^H(\widehat{\mathbf{W}}_1\widehat{\mathbf{C}}\widehat{\mathbf{W}}_1^H)^{-1}\widehat{\mathbf{W}}_1\widehat{\mathbf{C}}), \quad (24)$$

where \mathbf{Q} can be an arbitrary $(d - m) \times m$ full-row-rank matrix such that \mathbf{B} has full row-rank, meets the condition (23).

Now, to apply (7), $\widehat{\mathbf{A}}_1$ must be computed, which consists of first m columns of $\widehat{\mathbf{A}} = \widehat{\mathbf{W}}^{-1}$, so it satisfies

$$\widehat{\mathbf{W}}_1\widehat{\mathbf{A}}_1 = \mathbf{I}, \quad (25)$$

$$\mathbf{B}\mathbf{A}_1 = \mathbf{Q}(\mathbf{I} - \widehat{\mathbf{C}}\widehat{\mathbf{W}}_1^H(\widehat{\mathbf{W}}_1\widehat{\mathbf{C}}\widehat{\mathbf{W}}_1^H)^{-1}\widehat{\mathbf{W}}_1\widehat{\mathbf{C}})\widehat{\mathbf{A}}_1 = \mathbf{0}. \quad (26)$$

The latter equation is satisfied whenever $\widehat{\mathbf{A}}_1 = \widehat{\mathbf{C}}\widehat{\mathbf{W}}_1^H\mathbf{R}$ where \mathbf{R} is an $m \times m$ matrix. To satisfy also (25), $\mathbf{R} = (\widehat{\mathbf{W}}_1\widehat{\mathbf{C}}\widehat{\mathbf{W}}_1^H)^{-1}$. Finally,

$$\mathbf{S}_{\text{INV}}^1 = \widehat{\mathbf{A}}_1\widehat{\mathbf{W}}_1\mathbf{X} = \widehat{\mathbf{C}}\widehat{\mathbf{W}}_1^H(\widehat{\mathbf{W}}_1\widehat{\mathbf{C}}\widehat{\mathbf{W}}_1^H)^{-1}\widehat{\mathbf{W}}_1\mathbf{X}, \quad (27)$$

which allows us to conclude this section by the following proposition.

Proposition 5: Let $\widehat{\mathbf{W}}_i$ be a part of an estimated demixing matrix, $i \in \{1, 2\}$, and let A3 be assumed. Then,

$$\widehat{\mathbf{S}}_{\text{INV}}^i = \widehat{\mathbf{S}}_{\text{LS}}^i.$$

III. PERTURBATION ANALYSIS

Throughout this section, let \mathbf{W} denote the exact demixing transform, that is $\mathbf{W} = \mathbf{H}^{-1}$. We present an analysis of the sensor response estimators (7) and (14) when \mathbf{W} is known up to a small deviation². Let $\mathbf{V} = \mathbf{W} + \mathbf{\Xi}$ be the available observation of \mathbf{W} where $\mathbf{\Xi}$ is a ‘‘small’’ matrix; \mathbf{V}_1 will denote the sub-matrix of \mathbf{V} containing the first m rows; similarly $\mathbf{\Xi} = [\mathbf{\Xi}_1; \mathbf{\Xi}_2]$; $\mathbf{A} = \mathbf{V}^{-1}$ and \mathbf{A}_1 contains the first m columns of \mathbf{A} ; let also $\Delta\mathbf{C} = \widehat{\mathbf{C}} - \mathbf{C}$ be ‘‘small’’ and of the same asymptotic order as $\mathbf{\Xi}$ (typically, $\Delta\mathbf{C} = \mathcal{O}_p(N^{-1/2})$ where $\mathcal{O}_p(\cdot)$ is the stochastic order symbol).

Now, consider the transform matrices $\mathbf{T}_1 \triangleq \mathbf{A}_1 \mathbf{V}_1$ and $\mathbf{T}_2 \triangleq \widehat{\mathbf{C}} \mathbf{V}_1^H (\mathbf{V}_1 \widehat{\mathbf{C}} \mathbf{V}_1^H)^{-1} \mathbf{V}_1$ estimating \mathbf{S}^1 from \mathbf{X} , respectively. The analysis resides in the computation of their squared distances (the Frobenius norm) from the ideal transform, that is, from $\mathbf{H}_1 \mathbf{W}_1$. Using first-order expansions and neglecting higher-order terms, it is derived in Appendix that the following approximations hold.

$$\|\mathbf{H}_1 \mathbf{W}_1 - \mathbf{T}_1\|_F^2 \approx \|\mathbf{H} \mathbf{\Xi} \mathbf{H}_1 \mathbf{W}_1 - \mathbf{H}_1 \mathbf{\Xi}_1\|_F^2, \quad (28)$$

$$\begin{aligned} \|\mathbf{H}_1 \mathbf{W}_1 - \mathbf{T}_2\|_F^2 &\approx \left\| \mathbf{H}_1 (\mathbf{\Xi}_1 \mathbf{C} \mathbf{W}_1^H + \mathbf{W}_1 \mathbf{C} \mathbf{\Xi}_1^H) \mathbf{C}_{s_1}^{-1} \mathbf{W}_1 \right. \\ &\quad \left. (\mathbf{H}_1 \mathbf{W}_1 - \mathbf{I}) \Delta \mathbf{C} \mathbf{W}_1^H \mathbf{C}_{s_1}^{-1} \mathbf{W}_1 - \mathbf{H}_1 \mathbf{\Xi}_1 - \mathbf{C} \mathbf{\Xi}_1^H \mathbf{C}_{s_1}^{-1} \mathbf{W}_1 \right\|_F^2. \end{aligned} \quad (29)$$

To provide a deeper insight, we will analyze a particular case where $\mathbf{H} = \mathbf{W} = \mathbf{I}$, $\mathbf{C}_{s_1} = \sigma_1^2 \mathbf{I}$, and $\mathbf{C}_{s_2} = \sigma_2^2 \mathbf{I}$. Let the elements of $\mathbf{\Xi}$ all be independent random variables with zero mean such that the variance of each element of $\mathbf{\Xi}_i$ is equal to λ_i^2 . For further simplification, let the elements of $\Delta\mathbf{C}_{ij}$, which denotes the ij th block of $\Delta\mathbf{C}$, $i, j = 1, 2$, be also independent random variables whose variance is equal to $\sigma_i \sigma_j C$. Then, the expectation values of the right-hand sides of (28) and (29), respectively, are equal to

$$\mathbb{E} \left[\|\mathbf{H}_1 \mathbf{W}_1 - \mathbf{T}_1\|_F^2 \right] \approx (\lambda_1^2 + \lambda_2^2) m(d - m), \quad (30)$$

$$\mathbb{E} \left[\|\mathbf{H}_1 \mathbf{W}_1 - \mathbf{T}_2\|_F^2 \right] \approx \left[\left(1 + \frac{\sigma_2^2}{\sigma_1^2} \right) \lambda_1^2 + \frac{\sigma_2}{\sigma_1} C \right] m(d - m). \quad (31)$$

Comparing (30) and (31) shows the pros and cons of the estimators. The latter depends on σ_2^2/σ_1^2 , which reflects the ratio between the power of s_1 and that of s_2 . The expression (30) does not depend on this ratio explicitly³. For simplicity, let us assume that $\sigma_2^2/\sigma_1^2 = 1$.

Next, (31) depends on C while (30) is independent of it. Since C captures the covariance estimation error in $\Delta\mathbf{C}$, it typically decreases with the length of data N . Usually, C has asymptotic order $\mathcal{O}(N^{-1/2})$; see, e.g., Appendix A.B in [30]. For the sake of the analysis, we will assume that $C = 0$. Then, (31) changes to

$$\mathbb{E} \left[\|\mathbf{H}_1 \mathbf{W}_1 - \mathbf{T}_2\|_F^2 \right] \approx 2\lambda_1^2 m(d - m). \quad (32)$$

The expressions (30) and (32) point to the main difference of the estimators when $\mathbf{H} = \mathbf{W} = \mathbf{I}$: While the performance of INV depends on λ_1^2 and λ_2^2 , that of LS depends purely on λ_1^1 . In the special case $\lambda_1^1 = \lambda_2^1$, the performances coincide.

²The analysis of (12) follows from that of (14) when $\Delta\mathbf{C} = \mathbf{0}$.

³Typically, there is an implicit dependency of the estimation error $\mathbf{\Xi}$ on σ_2^2/σ_1^2 . Therefore, λ_1^2 as well as λ_2^2 are influenced by σ_1^2 and σ_2^2 .

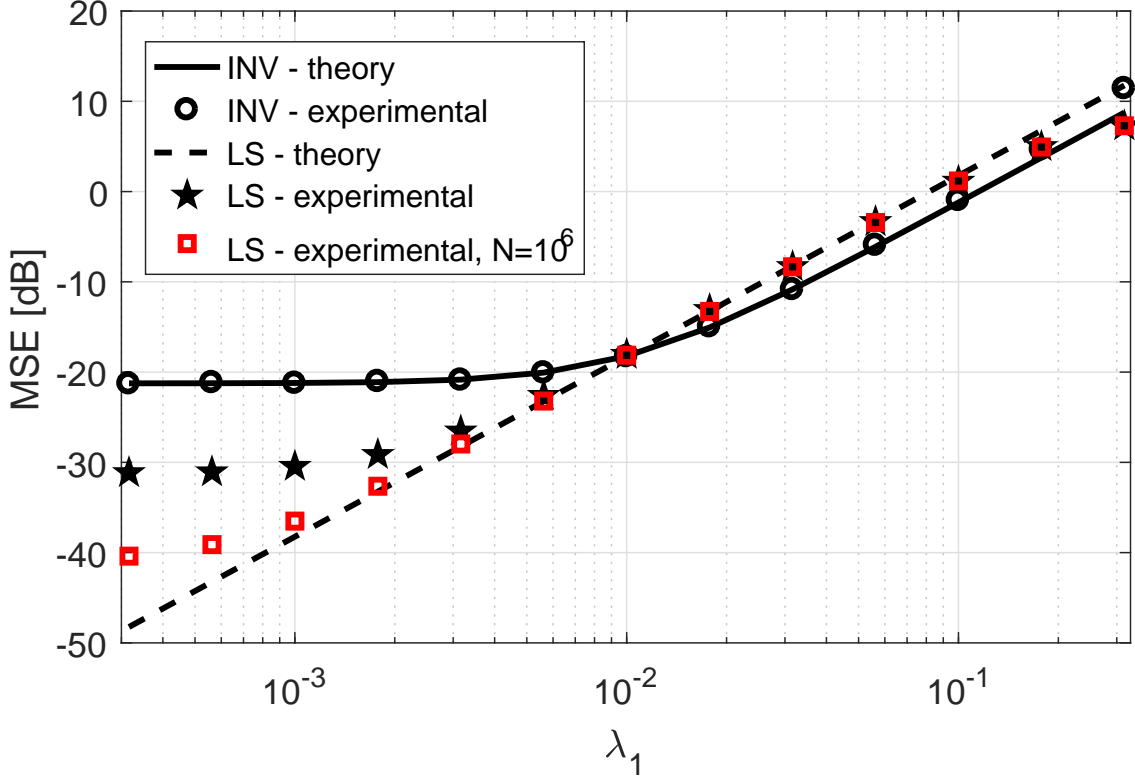


Fig. 1. Comparison of theoretical and experimental mean square error of INV and LS when $d = 20$, $m = 5$, $\mathbf{H} = \mathbf{W} = \mathbf{I}$, $\sigma_1^2 = \sigma_2^2 = 1$, $C = 0$, $N = 10^5$, $\lambda_2^2 = 10^{-4}$.

To verify the theoretical expectations, we conducted a simple simulation where $d = 20$, $m = 5$, $\mathbf{H} = \mathbf{W} = \mathbf{I}$, $\sigma_1^2 = \sigma_2^2 = 1$, $C = 0$, $N = 10^5$, $\lambda_2^2 = 10^{-4}$. Ξ and \mathbf{S} were drawn from complex Gaussian distribution with zero mean and unit variance. The average squared errors of INV and LS averaged over 100 trials for each value of λ_1 are compared, respectively, with the expressions (30) and (32) in Fig 1.

The theoretical error of INV is in a good agreement with the experimental one for all values of λ_1 . The same holds for that of LS until $\lambda_1 \geq 0.003$. For smaller values of λ_1 , the experimental error of LS is limited while the theoretical one is decreasing. This is caused by the influence of $\Delta\mathbf{C}$, which is fully neglected in (32) and modeled through C in (31). The experimental error of LS evaluated for $N = 10^6$ confirms that (31) is a more accurate theoretical error of LS than (32).

In this example, INV outperforms LS when $\lambda_1 > \lambda_2$, and vice versa. However, these results are valid only in the special case when $\mathbf{H} = \mathbf{W} = \mathbf{I}$. Simulations in Section V consider general mixing matrices, thereby compare the estimators in more realistic situations.

IV. NOISE EXTRACTION FROM UNDERDETERMINED MIXTURES

A. Mixture Model

Now we focus on a more realistic scenario that appears in most array processing problems. Let the mixture be described as

$$\mathbf{x} = \mathbf{H}_1 \mathbf{s}_1 + \mathbf{s}_2, \quad (33)$$

where \mathbf{H}_1 is a $d \times m$ matrix having full column rank, \mathbf{s}_1 is an $m \times 1$ vector of target components, and \mathbf{s}_2 is a $d \times 1$ vector of noise signals. Note that, in this model, \mathbf{s}_2 is simultaneously equal to \mathbf{s}^2 .

The mixture model corresponds with (1), but \mathbf{H} is equal to $[\mathbf{H}_1 \mathbf{I}_{d \times d}]$ and has dimensions $d \times (m + d)$, which makes the problem underdetermined ($r = m + d$).

In general, a linear transform that separates \mathbf{s}_1 or \mathbf{s}_2 from \mathbf{x} does not exist, unless (33) is implicitly regular (e.g., when $\mathbf{C}_{\mathbf{s}_2}$ has rank $d - m$)⁴. From now on, we focus on the difficult case where, generally speaking, neither \mathbf{s}_1 nor \mathbf{s}_2 can be separated.

B. Target Signal Cancellation and Noise Extraction

Since the separation of \mathbf{s}_1 is not possible, multichannel noise reduction systems follow an inverse approach: the target components \mathbf{s}_1 are first linearly canceled from the mixture in order to estimate a reference of the noise components \mathbf{s}_2 . Second, a linear transform or adaptive filtering is used to subtract the noise from the mixture as much as possible; see, e.g., [37], [38], [39], [40], [42], [43].

Specifically, the cancellation of the target component is achieved through a matrix \mathbf{W} such that

$$\mathbf{W}\mathbf{H}_1 = \mathbf{0}. \quad (34)$$

Since \mathbf{H}_1 has rank m , the maximum possible rank of \mathbf{W} is $d - m$, which points to the fundamental limitation: The maximum dimension of the subspace spanned by the extracted noise signals $\mathbf{W}\mathbf{x} = \mathbf{W}\mathbf{s}_2$ is $d - m$.

Assume for now that any $(d - m) \times d$ matrix \mathbf{W} having full row-rank has been identified (e.g., using BSS). To estimate \mathbf{s}_2 , LS can be used (INV cannot be applied in the underdetermined case), so

$$\hat{\mathbf{s}}_{\text{LS}}^2 = \mathbf{C}\mathbf{W}^H(\mathbf{W}\mathbf{C}\mathbf{W}^H)^{-1}\mathbf{W}\mathbf{x}, \quad (35)$$

or

$$\hat{\mathbf{S}}_{\text{LS}}^2 = \hat{\mathbf{C}}\mathbf{W}^H(\mathbf{W}\hat{\mathbf{C}}\mathbf{W}^H)^{-1}\mathbf{W}\mathbf{X}. \quad (36)$$

Proposition 6: Let \mathbf{W} be a $(d - m) \times d$ transform matrix having rank $d - m$ and satisfying (34), and let \mathbf{Q} denote a $d \times (d - m)$ matrix. Under A2, $\hat{\mathbf{s}}_{\text{LS}}^2$ is a minimizer of

$$\min_{\hat{\mathbf{s}}=\mathbf{Q}\mathbf{W}\mathbf{x}} \mathbb{E} [\|\mathbf{s}_2 - \hat{\mathbf{s}}\|^2]. \quad (37)$$

Assuming (6), $\hat{\mathbf{S}}_{\text{LS}}^2$ is a minimizer of

$$\min_{\hat{\mathbf{S}}=\mathbf{Q}\mathbf{W}\mathbf{X}} \|\mathbf{S}_2 - \hat{\mathbf{S}}\|_F^2. \quad (38)$$

⁴For example, model (33) is often studied under the assumption that at most d signals out of \mathbf{s}_1 and \mathbf{s}_2 are active at a given time instant; see, e.g. [35], [36].

Proof: Under A2 it holds that

$$\min_{\hat{\mathbf{s}}=\mathbf{Q}\mathbf{W}\mathbf{x}} \mathbb{E} [\|\mathbf{s}_2 - \hat{\mathbf{s}}\|^2] = \min_{\hat{\mathbf{s}}=\mathbf{Q}\mathbf{W}\mathbf{x}} \mathbb{E} [\|\mathbf{x} - \hat{\mathbf{s}}\|^2].$$

When (6) holds, then

$$\min_{\hat{\mathbf{s}}=\mathbf{Q}\mathbf{W}\mathbf{x}} \|\mathbf{S}_2 - \hat{\mathbf{S}}\|_F^2 = \min_{\hat{\mathbf{s}}=\mathbf{Q}\mathbf{W}\mathbf{x}} \|\mathbf{X} - \hat{\mathbf{S}}\|_F^2.$$

The statements of the proposition follow, respectively, by the definitions (12) and (14). \blacksquare

The latter proposition points to important limitations of LS that should be taken into account in the underdetermined scenario. First, LS estimates a d -dimensional signal only from a $(d-m)$ -dimensional signal subspace. Second, (35) is optimal under A2 in the least-squares sense of (37). Third, (36) is optimal in the sense of (38) only when (6) is valid, which is much stronger assumption than A2.

V. SIMULATIONS

This section is devoted to extensive Monte Carlo simulations where the signals and system parameters are randomly generated. Real and complex parts of random numbers are always generated independently according to the Gaussian law with zero mean and unit variance. Each trial of a simulation consists of the following steps.

- 1) The dimension parameters d and m are chosen.
- 2) N samples of the original components \mathbf{s}_1 and \mathbf{s}_2 are randomly generated according to the Gaussian law.
- 3) The mixing matrix \mathbf{H} is generated, $\mathbf{W} = \mathbf{H}^{-1}$, $\mathbf{X} = \mathbf{H}\mathbf{S}$, and $\hat{\mathbf{C}} = \mathbf{X}\mathbf{X}^H/N$.
- 4) The estimation of \mathbf{W} is simulated by adding random perturbations to its blocks, that is, $\widehat{\mathbf{W}}_1 = \mathbf{W}_1 + \mathbf{\Xi}_1$ and $\widehat{\mathbf{W}}_2 = \mathbf{W}_2 + \mathbf{\Xi}_2$, where the elements of $\mathbf{\Xi}_1$ and $\mathbf{\Xi}_2$ have, respectively, variances λ_1^2 and λ_2^2 ; $\widehat{\mathbf{W}} = [\widehat{\mathbf{W}}_1 \widehat{\mathbf{W}}_2]^5$. Then, $\widehat{\mathbf{W}}_1$ and $\widehat{\mathbf{W}}_2$ are multiplied by random regular scaling matrices of corresponding dimensions.
- 5) The accuracy of the INV and LS estimates of \mathbf{S}^1 using $\widehat{\mathbf{W}}$ is evaluated through the normalized mean-squared error defined as

$$\text{NMSE}_j = \frac{\|\mathbf{H}_1 \mathbf{W}_1 - \mathbf{T}_j\|_F^2}{\|\mathbf{H}_1 \mathbf{W}_1\|_F^2}, \quad (39)$$

$$j = 1, 2.$$

The following subsection reports results of simulations assuming the determined model. The next subsection considers the underdetermined model (33).

A. Determined model

1) *Influence of the Estimation Errors in $\widehat{\mathbf{W}}$:* The experiment is done with $d = 5$, $m = 2$, and $N = 10^4$; λ_2^2 is equal to one of four constants (10^{-1} , 10^{-2} , 10^{-3} , and 10^{-4}) while λ_1^2 is varied. Each simulation is repeated in 10^5 trials. The average NMSE achieved by INV and LS are shown in Fig. 2.

The results of INV are highly influenced by λ_2^2 that controls the perturbation of $\widehat{\mathbf{W}}_2$. For example, for $\lambda_2^2 = 10^{-1}$ and $\lambda_2^2 = 10^{-2}$, INV fails in the sense that the achieved NMSE is above 0 dB. This happens even

⁵Note that $\widehat{\mathbf{W}}_1$ and $\widehat{\mathbf{W}}_2$ are not constrained to satisfy A3. Otherwise, the comparison of INV and LS would not give a sense due to Proposition 5.

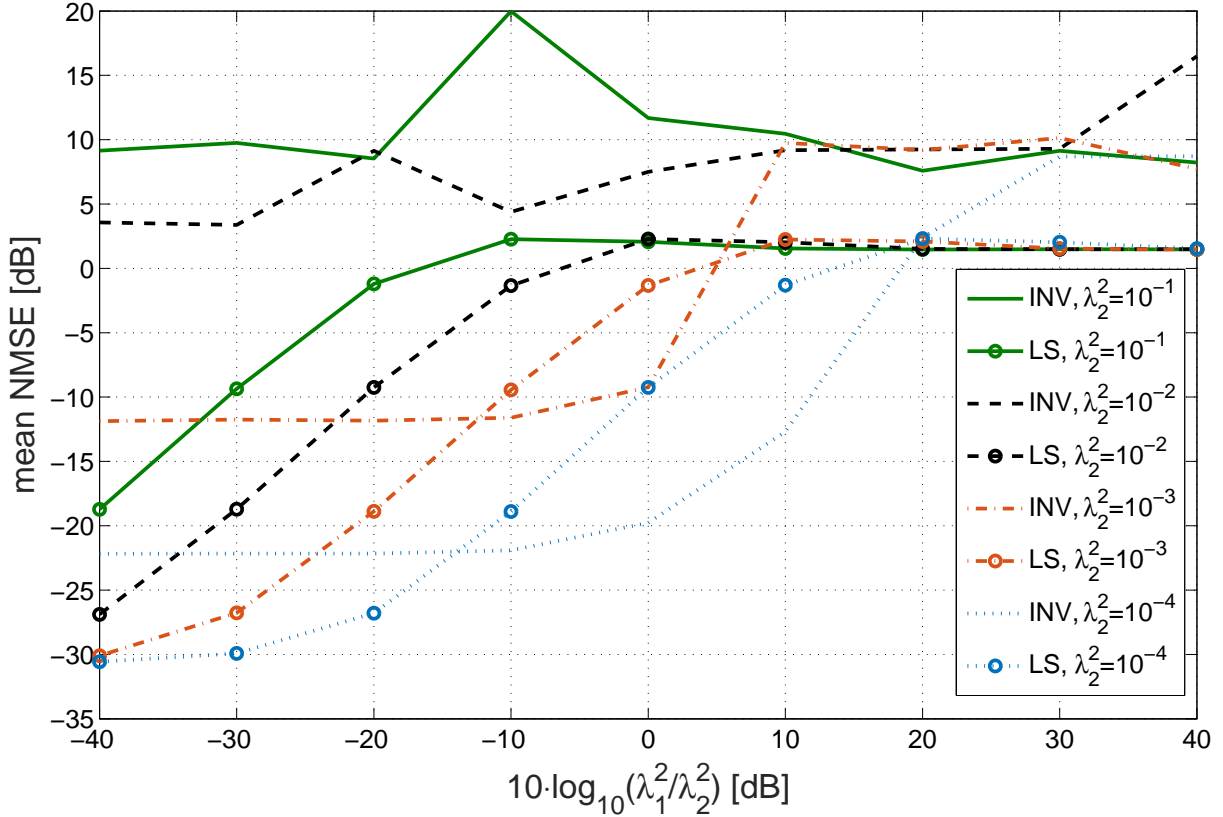


Fig. 2. NMSE averaged over 10^5 trials where $d = 5$, $m = 2$, $N = 10^4$, λ_2^2 is fixed, and λ_1^2 is varied.

if λ_1^2 , which controls the perturbation of $\widehat{\mathbf{W}}_1$, is relatively “small”. For $\lambda_2^2 = 10^{-3}$ and $\lambda_2^2 = 10^{-4}$, the NMSE of INV decreases with decreasing λ_1^2 . However, the NMSE is lower bounded (does not improve as $\lambda_1^2 \rightarrow 0$). All these results point to the dependency of INV on $\widehat{\mathbf{W}}_2$.

The NMSE of LS depends purely on λ_1^2 . It is always improved with the decreasing value of λ_1^2 (it is only limited by the length of data which influences the accuracy of the sample covariance matrix $\widehat{\mathbf{C}}$). In this experiment, LS is outperformed by INV only in a few cases, namely, when $\lambda_2^2 = 10^{-4}$ and λ_1^2/λ_2^2 is higher than -14 dB. INV thus appears to be beneficial compared to LS in situations where the whole $\widehat{\mathbf{W}}$ is a sufficiently accurate estimate of \mathbf{W} .

2) *Varying Dimension*: In the situation here, the target component s_1 has dimension one, i.e., $m = 1$, while the dimension of the mixture d is changed from 2 through 20; $N = 10^4$. The variances λ_1^2 and λ_2^2 are fixed, namely, $\lambda_2^2 = 10^{-3}$ and λ_1^2 is chosen such that $10 \log_{10} \lambda_1^2/\lambda_2^2$ corresponds, respectively, to -10 , 0 , and 10 dB. The NMSE averaged over 10^5 trials is shown in Fig. 3.

The NMSE values of both methods are increasing with growing d . In the INV case, the NMSE grows smoothly until it reaches a certain threshold value of d . The experiments show that this threshold depends on λ_1^2 and λ_2^2 . Above this threshold, the NMSE of INV abruptly grows. It points to a higher sensitivity of INV to the estimation errors in $\widehat{\mathbf{W}}$ when the dimension of data is “high”.

LS yields smooth and monotonic behavior of NMSE for every d . It is outperformed by INV if both λ_1^2 and

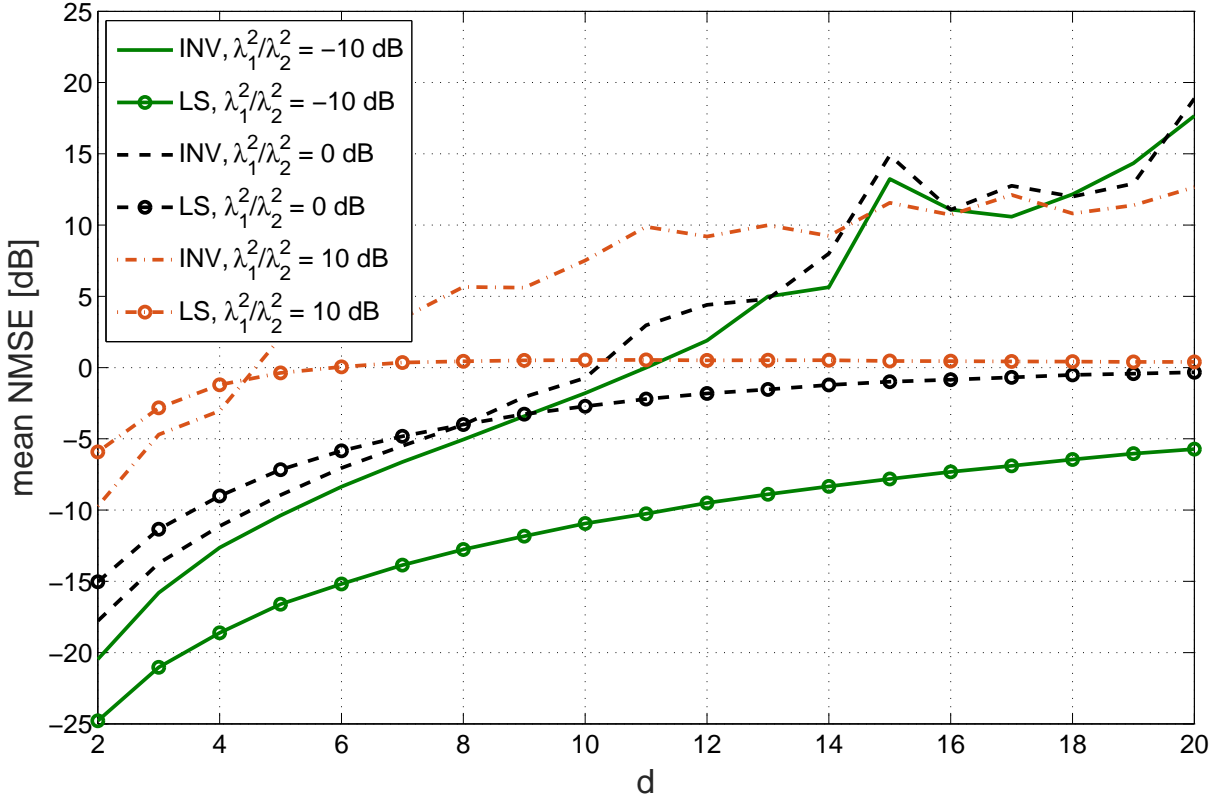


Fig. 3. NMSE averaged over 10^5 trials as a function of $d = 2, \dots, 20$; here $m = 1$, $\lambda_2^2 = 10^{-3}$, and $N = 10^4$.

λ_2^2 as well as the data dimension d are sufficiently small.

3) *Target Component Dimension*: The dimension of the mixture d is now put equal to 20, while the dimension of the target component m is varied from 1 through $d - 1$. Results for three different choices of λ_1^2 and λ_2^2 are shown in Fig. 4. The scenario with $\lambda_1^2 = \lambda_2^2 = 10^{-3}$ appears to be difficult for both methods as they do not achieve NMSE below 0 dB. INV also fails when $\lambda_2^2 = 10^{-3}$ and λ_1^2/λ_2^2 corresponds to -10 dB (i.e., $\lambda_1^2 = 10^{-4}$) until $m \leq 17$. This is in accordance with the results of the previous example that shows that INV fails when λ_1^2 , λ_2^2 and d are “too large”. The example here reveals one more detail: INV can benefit from smaller perturbations of the target component ($\lambda_1^2 = 10^{-4}$) even if λ_2^2 is larger, but the target dimension must be large enough with respect to d .

LS performs independently of λ_2^2 , which is confirmed by the cases that are plotted with solid and dashed lines in Fig. 4: these lines coincide as both correspond to the same λ_1^2 (although different λ_2^2). LS is outperformed by INV when $\lambda_1^2 = \lambda_2^2 = 10^{-4}$, which, again, occurs when the estimation error of the whole $\widehat{\mathbf{W}}$ is very small.

B. Underdetermined model

In the example of this subsection, we consider the underdetermined mixture model (33) where $m = 1$, $d = 2, \dots, 20$, and $N = 50, \dots, 10^5$. The goal is to examine the reconstruction of the noise components \mathbf{S}_2 through (36). \mathbf{H}_1 is randomly generated. Then, \mathbf{W} is such that its rows form a basis of the $(d - m)$ -dimensional subspace that is orthogonal to \mathbf{H}_1 plus a random Gaussian perturbation matrix whose elements have the variance

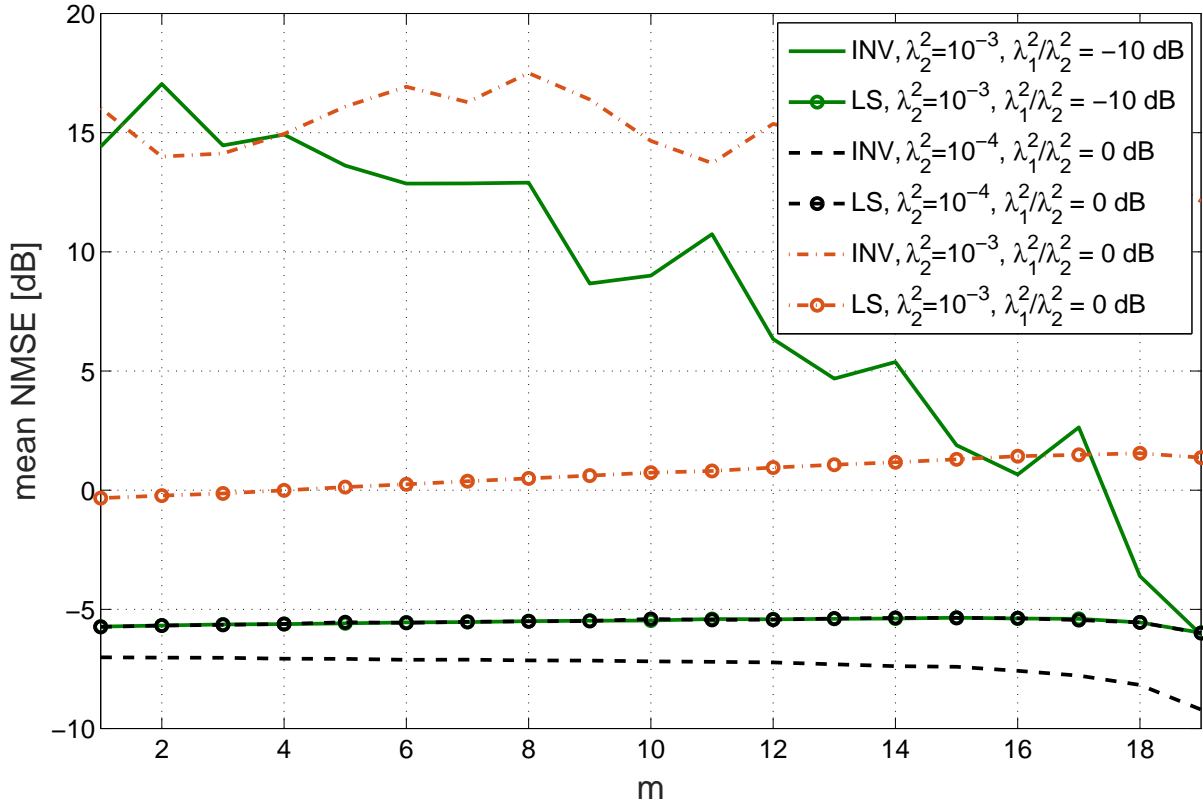


Fig. 4. NMSE averaged over 10^5 trials where $d = 20$, $N = 10^4$, and $m = 1, \dots, 19$.

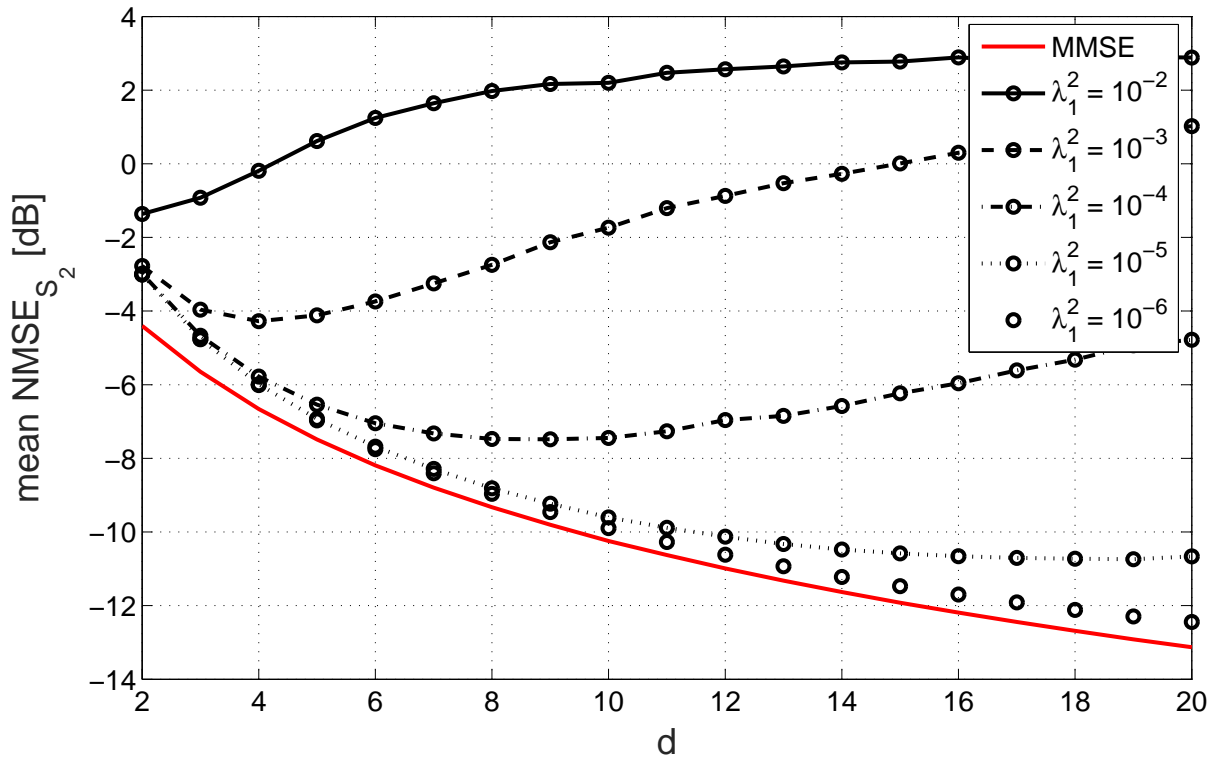


Fig. 5. Average NMSE_{S_2} as a function of d achieved by (35) in an experiment with the underdetermined model (33); $m = 1$; $N = 10^4$. MMSE denotes the NMSE achieved by the optimum minimum mean-squared error solution (41). The signals are generated as random complex Gaussian i.i.d.

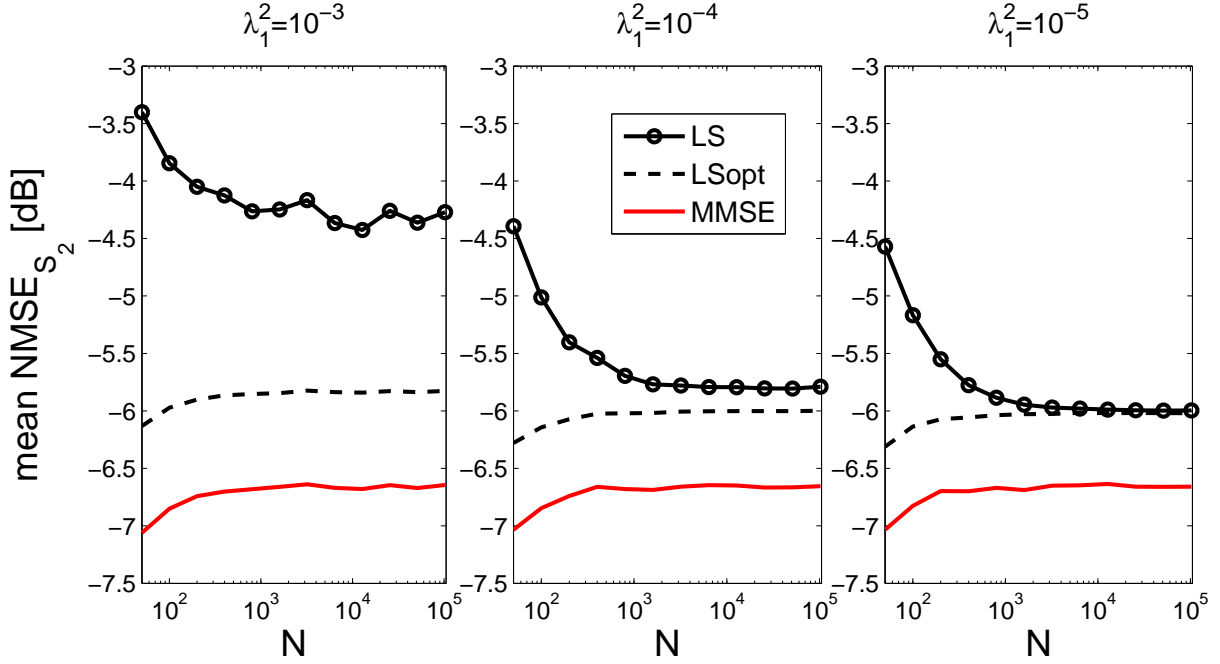


Fig. 6. Average NMSE_{S_2} as a function of N achieved through (36), (38) and (14); $d = 4$; $\lambda_1^2 = 10^k$, $k = -3, -4, -5$.

values equal to $\lambda_1^2 = 10^k$, $k = -2, -3, \dots, -6$, respectively. After applying (36), the evaluation is done using the normalized mean square distance

$$\text{NMSE}_{S_2} = \frac{\|S_2 - \widehat{S}_2\|_F^2}{\|S_2\|_F^2}. \quad (40)$$

Owing to the statement of Proposition 6, it is worth comparing \widehat{S}_2 with the exact solution of (38), which will be abbreviated by LSopt, and with the minimum mean square error solution, marked as MMSE, defined as the minimizer of

$$\min_{Q \in \mathbb{C}^{d \times d}} \|S_2 - QX\|_F^2. \quad (41)$$

The latter gives the minimum achievable value of NMSE_{S_2} by a linear estimator; cf. (38) and (14).

The results averaged over 10^3 independent trials are shown in Figures 5 and 6. Fig. 5 shows results for $N = 10^4$. One observation here is that NMSE_{S_2} achieved through LS is getting closer to that of MMSE as λ_1^2 approaches zero. Next, NMSE_{S_2} improves with growing dimension d , but it appears that it stops improving at a certain d and grows beyond this threshold value, which depends on λ_1^2 . For example, when $\lambda_1^2 = 10^{-4}$, the NMSE_{S_2} is decaying until $d = 8$ and grows beyond $d \geq 10$.

Fig. 6 shows NMSE_{S_2} as a function of N when $d = 4$. This detailed observation shows that LS approaches LSopt as N grows and λ_1^2 approaches zero, but does not achieve the performance of MMSE. This is the fundamental limitation due to the dimension of the separable signal subspace, that is, $d - m$.

VI. PRACTICAL EXAMPLES

A. De-noising of Electrocardiogram

Fig. 7 shows two seconds of a recording from a three channel electrocardiogram (ECG) of a Holter monitor, which was sampled at 500 Hz. The recording is strongly interfered with a noise signal originating from the Holter display. The fundamental frequency of the noise is about 37 Hz, and the noise contains several harmonics.

Since the noise is significantly stronger than the ECG components, Principal Component Analysis (PCA) can be used to find a demixing transform that separates the noise from the mixture. Therefore, we take the eigenvector corresponding to the highest eigenvalue of the covariance matrix of the recorded data (the principal vector) as the separating transform. Then, the noise responses on the electrodes are computed using LS and subtracted from the original noisy recording. This approach is computationally cheaper than doing the whole PCA and using INV then. According to Proposition 5, both approaches give the same result as PCA yields component that are exactly orthogonal.

To compare, we repeated the same experiment using the vector obtained through Independent Component Analysis (ICA). One-unit FastICA [15] with $\tanh(\cdot)$ nonlinearity was used to compute the vector separating the noise component. To avoid the permutation ambiguity, the algorithm was initialized from $[1\ 1\ 1]$, because the noise appears to be uniformly distributed over the electrodes. Also here the approach is faster than doing the whole orthogonally-constrained ICA (e.g. using Symmetric FastICA) and using INV.

Figures 8 and 9 show the resulting signals where the estimated images of the noise component were removed, respectively, through PCA and ICA. Both results show very efficient subtraction of the noise. A visual inspection of the detail in Fig. 8 shows certain residual noise that does not appear in Fig. 9, so the separation through ICA appears to be more accurate than by PCA. Combining one-unit ICA algorithm with LS, the computational complexity of the ICA solution is decreased.

B. Blind Separation with Incomplete Demixing Transforms

Proposition 5 points to the fact that if BSS is based on a method that yields (almost) orthogonal estimates of s_1 and s_2 , INV and LS are principally not that different. The example of this section demonstrates a situation where the estimates are significantly nonorthogonal, so INV and LS yield considerably different results.

Recently, a novel approach for blind separation of convolutive mixtures of audio signals has been proposed in [45], [47]. The idea resides in the application of IVA in the frequency-domain on a constrained subset of frequencies where the input (mixed) signals are active. This is in contrast with the conventional Frequency-Domain IVA (ICA), which is applied in all frequencies. The motivation behind is threefold: computational savings, improved accuracy (especially in environments with sparse room impulse responses), and the prediction of complete demixing transform for separation of future signals whose activity appears in other frequencies.

The method proceeds in three main steps. First, the subset \mathcal{S} of p percents of the most active frequency bins is selected. This can be done through estimating the power spectrum of the signal on a reference microphone using the coefficients of its short-term Fourier transform. The frequency bins with maximum average magnitude of Fourier coefficients are selected. Second, an IVA method is applied that estimates the demixing matrices

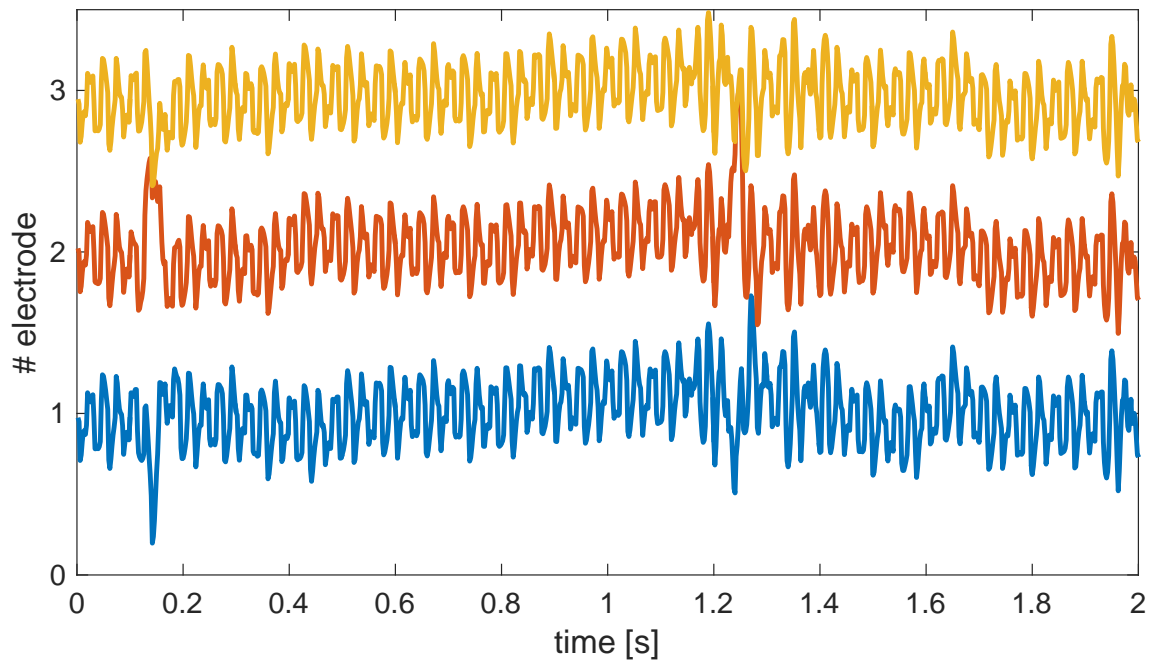


Fig. 7. A two-second sample of a three channel electrocardiogram interfered by a noise signal originating from a Holter display.

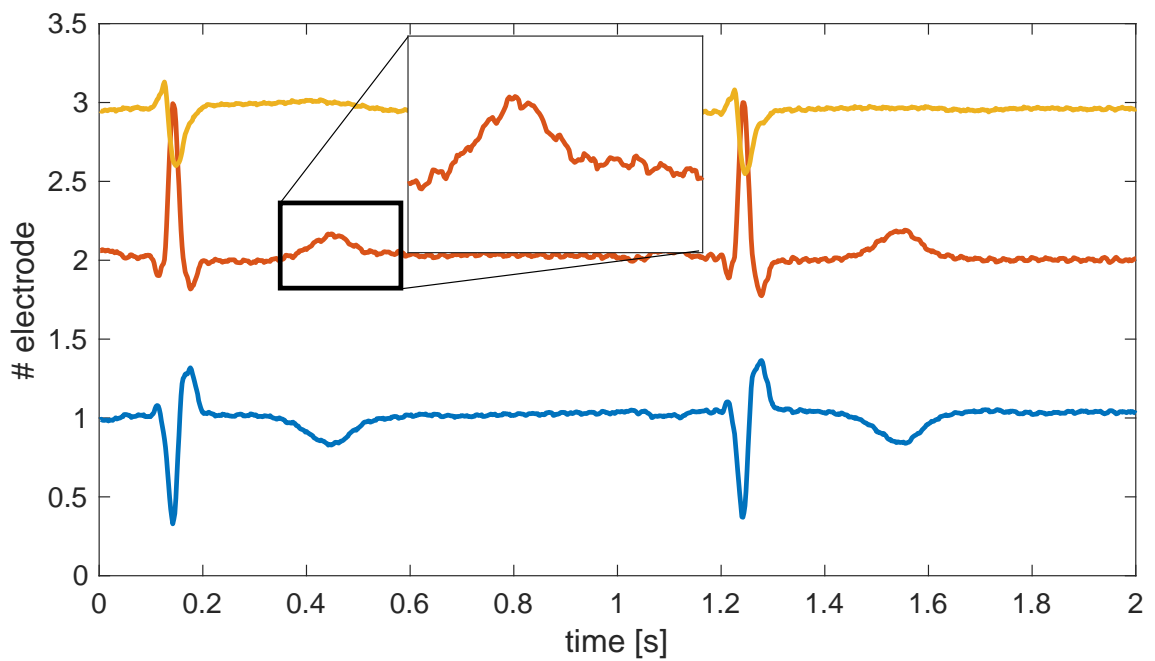


Fig. 8. Cleaned data from Fig. 7 after the subtraction of noise responses that were estimated through the main principal component and LS.

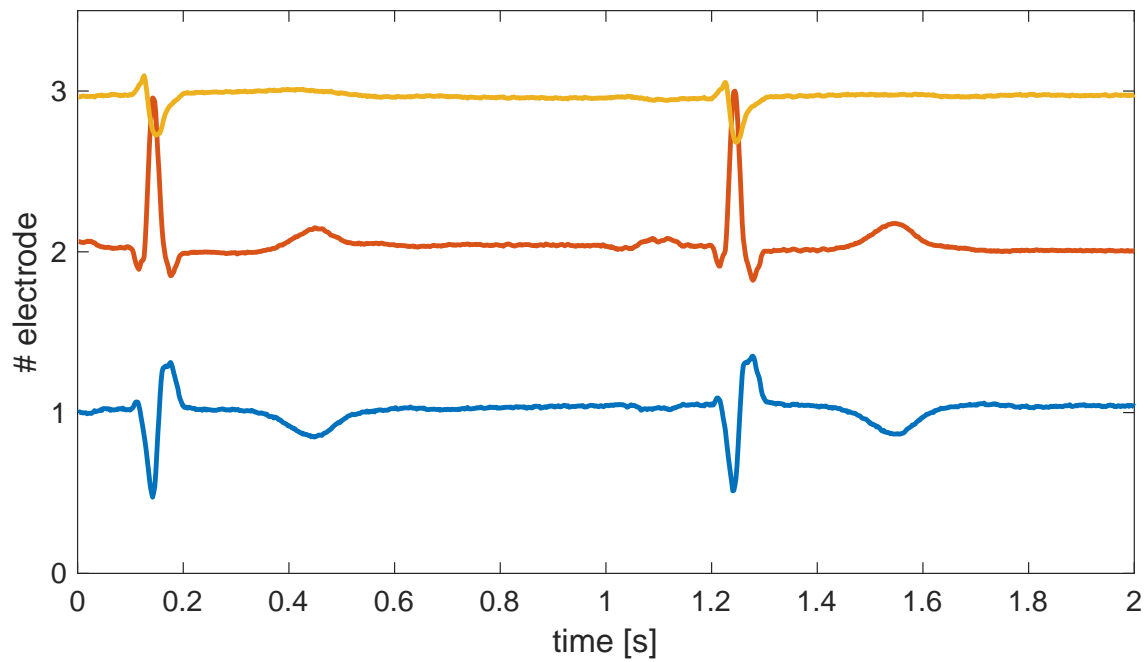


Fig. 9. Cleaned data from Fig. 7 after the subtraction of noise images that were estimated using the one-unit FastICA and LS.

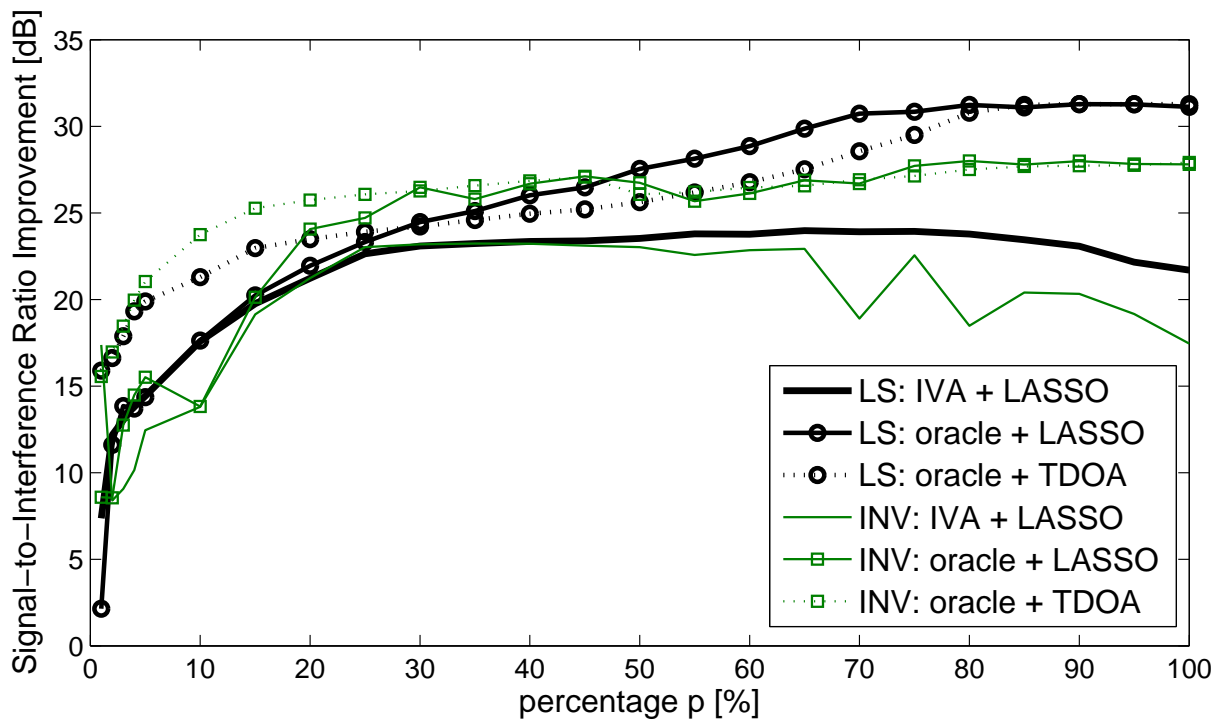


Fig. 10. Improvement of signal-to-interference ratio as a function of p , i.e., of percents of selected active frequencies in \mathcal{S} for the estimation of incomplete demixing transform. The evaluation was performed on speech signals.

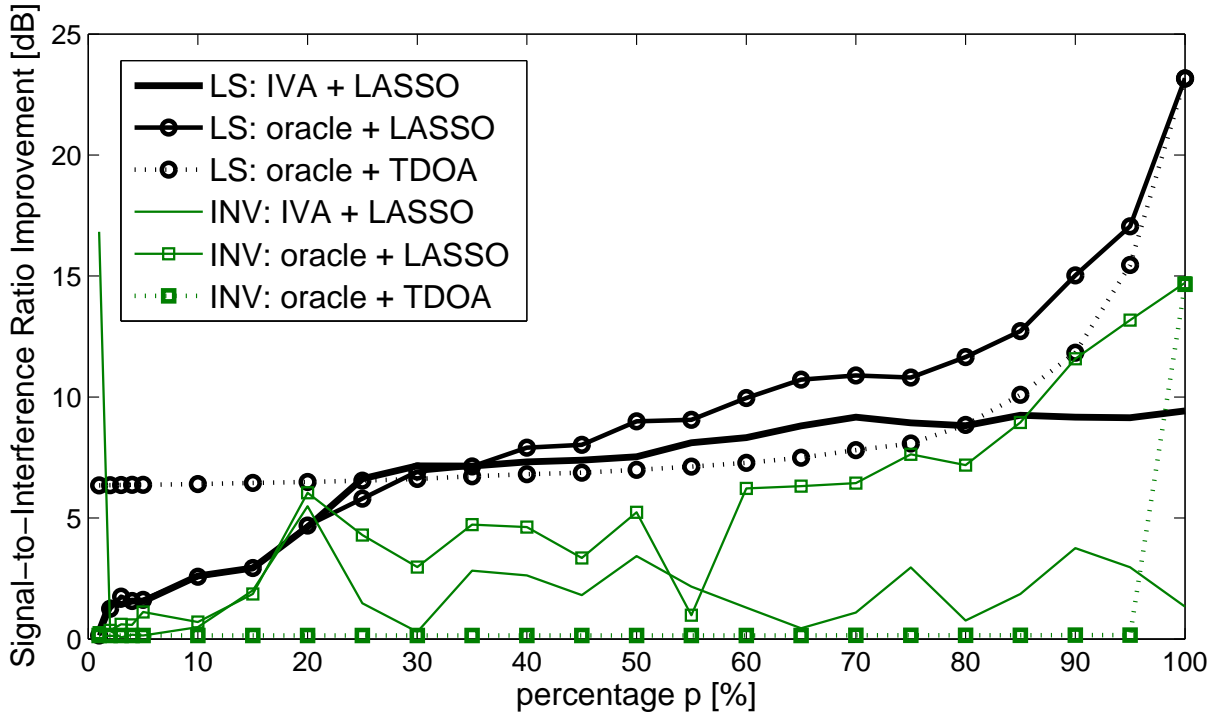


Fig. 11. Improvement of signal-to-interference ratio as a function of p . The evaluation was performed on white noise signals that uniformly excite the whole frequency range.

within the subset of the selected frequencies. The subset of the matrices is referred to as Incomplete Demixing Transform (IDT). Third, the IDT is completed by a given method.

We consider the same experiment with two simultaneously speaking persons and two microphones as in [45]. Signals have 10 seconds in length; the sampling frequency is 16 kHz. The signals are convolved with room impulse responses (RIR) generated by a simulator and mixed together. Reflection order is set to 1 so that the RIRs are significantly sparse (the results of this experiment with reflection order 10 when RIRs are no more sparse are available in [45]). Then, the signals are transformed into the short-term Fourier domain with the window length of 1024 samples and shift 128. The convolution is, in the frequency domain, approximated by the set of multiplicative models (1) where $d = r = 2$ where one model corresponds to one frequency bin; there are 513 models in total.

As for the second step, the demixing matrices are estimated from the mixed signals using the natural gradient algorithm for IVA [25] applied to the subset of models (1). To compare, “oracle” demixing matrices are derived on \mathcal{S} using known responses of the speakers. This gives the IDT that is known only on the selected subset \mathcal{S} .

The IDT is completed by two alternative methods. The first method, denoted as TDOA, utilizes known time-differences of arrival of the signals. The unknown demixing matrices are such that their rows correspond to the null beamformer steering spatial null towards the unwanted speaker. The second approach, denoted as LASSO, completes the IDT through finding the sparsest representations of incomplete relative transfer functions (RTF)

that are derived from the IDT⁶. Let \mathbf{q} denote an $|\mathcal{S}| \times 1$ vector that collects the coefficients of an incomplete RTF; $|\mathcal{S}|$ is the number of elements in \mathcal{S} . The completed RTF is obtained as the solution of [46]

$$\arg \min_{\mathbf{h}} \|\mathbf{h}_{\mathcal{S}} - \mathbf{q}\|^2 + \epsilon \|\mathbf{F}^H \mathbf{h}\|_1, \quad (42)$$

where $\epsilon > 0$ controls the time-domain sparsity of the solution, \mathbf{F} is the matrix of the DFT, the subscript $(\cdot)_{\mathcal{S}}$ denotes a vector/matrix with selected elements/rows whose indices are in \mathcal{S} , and $\|\cdot\|_1$ denotes the ℓ_1 -norm.

Now, it is worth noting that the separated components by the demixing matrices after the completion can be significantly nonorthogonal. While the IVA applied within \mathcal{S} aims to find independent (thus ‘‘almost’’ or fully orthogonal) components, the method for the IDT completion does not take any regard to the orthogonality⁷.

Figures 10 and 11 show results of the experiment from [45] evaluated in terms of the Signal-to-Interference Ratio Improvement (SIR) after the signals are separated as a function of p (the percentage of frequencies in \mathcal{S}). In Fig. 10, the evaluation is performed with the speech signals, while Fig. 11 shows the results achieved as if the sources were white Gaussian sequences. The purpose of the latter evaluation is to evaluate the completed IDT uniformly over the whole frequency range, i.e., also in frequencies that were not excited by the speech signals. Note that SIR must be evaluated after resolving the scaling ambiguity in each frequency [41]. This gives us the opportunity to apply either INV or LS.

The results in Figures 10 and 11 point to significant differences between LS and INV in this evaluation. The results by LS appear to be less biased and stable as compared to those by INV, and can be interpreted in accord with the theory. In particular, LS shows that oracle+LASSO (oracle IDT completed by LASSO) outperforms oracle+TDOA for p between 35% and 80%. This gives sense, because LASSO can better exploit the sparsity of the RIRs generated in this experiment. The results by INV do not reveal this important fact. Next, LS shows in Fig. 10 that IVA+LASSO can improve the separation of the speech signals when $p < 100\%$. The evaluation on white noise in Fig. 11 shows that the loss of SIR is not essential until $p < 30\%$. The latter conclusion cannot be drawn with the results by INV.

VII. CONCLUSIONS

We have analyzed and compared two estimators of sensor images (responses) of sources that were separated from a multichannel mixture up to an unknown scaling factor: INV and LS. Simulations and perturbation analysis have shown pros and cons of the methods, which can be summarized into the following recommendations.

- LS is more practical in a sense that the whole mixing matrix need not be identified for its use, which is useful especially in underdetermined scenarios.
- The advantage of INV resides in the independence on the (estimated) covariance matrix.
- INV could be beneficial as compared to LS when used with non-orthogonal BSS algorithms, i.e., those not applying the orthogonal constraint. However, both the target as well as the interference subspaces must be estimated with a sufficient accuracy.

⁶As pointed in [45], LASSO could be seen as a generalization of TDOA, because impulse responses corresponding to null beamformers are pure-delay filters, which are perfectly sparse.

⁷The orthogonal constraint cannot be imposed within the frequencies outside of the set \mathcal{S} , because signals are not (or purely) active there.

Both approaches have been shown to be equivalent under the orthogonal constraint, so the differences in their accuracies are less significant when BSS yields signal components that are (almost) orthogonal (e.g. PCA, ICA, IVA). By contrast, the differences between the reconstructed images of nonorthogonal components can be large, as demonstrated in the example of Section VI-B.

APPENDIX: ASYMPTOTIC EXPANSIONS

Computation of (28)

Let \mathbf{E} contain first m columns of the $d \times d$ identity matrix. It follows that

$$\begin{aligned} \mathbf{H}\mathbf{E} &= \mathbf{H}_1, & \mathbf{A}\mathbf{E} &= \mathbf{A}_1, \\ \mathbf{E}^H\mathbf{W} &= \mathbf{W}_1, & \mathbf{E}^H\mathbf{V} &= \mathbf{V}_1. \end{aligned}$$

To derive an approximate expression for \mathbf{A} , we will use the first-order expansion

$$\mathbf{A} = \mathbf{V}^{-1} = (\mathbf{W} + \mathbf{\Xi})^{-1} = (\mathbf{I} + \mathbf{H}\mathbf{\Xi})^{-1}\mathbf{H} \quad (43)$$

$$\approx (\mathbf{I} - \mathbf{H}\mathbf{\Xi})\mathbf{H} = \mathbf{H} - \mathbf{H}\mathbf{\Xi}\mathbf{H}. \quad (44)$$

Now we apply this approximation and neglect terms of higher than the first order.

$$\begin{aligned} \|\mathbf{H}_1\mathbf{W}_1 - \mathbf{A}_1\mathbf{V}_1\|_F^2 &= \|\mathbf{H}_1\mathbf{W}_1 - \mathbf{A}\mathbf{E}\mathbf{E}^H\mathbf{V}\|_F^2 \approx \\ &= \|\mathbf{H}_1\mathbf{W}_1 - (\mathbf{H} - \mathbf{H}\mathbf{\Xi}\mathbf{H})\mathbf{E}\mathbf{E}^H(\mathbf{W} + \mathbf{\Xi})\|_F^2 = \\ &= \|\mathbf{H}_1\mathbf{W}_1 - (\mathbf{H}_1 - \mathbf{H}\mathbf{\Xi}\mathbf{H}_1)(\mathbf{W}_1 + \mathbf{\Xi}_1)\|_F^2 \approx \\ &= \|\mathbf{H}\mathbf{\Xi}\mathbf{H}_1\mathbf{W}_1 - \mathbf{H}_1\mathbf{\Xi}_1\|_F^2. \quad (45) \end{aligned}$$

■

Computation of (29)

We start with the first approximation

$$\begin{aligned} \left\| \mathbf{H}_1\mathbf{W}_1 - \widehat{\mathbf{C}}\mathbf{V}_1^H(\mathbf{V}_1\widehat{\mathbf{C}}\mathbf{V}_1^H)^{-1}\mathbf{V}_1 \right\|_F^2 &= \\ &= \left\| \mathbf{H}_1\mathbf{W}_1 - (\mathbf{C} + \Delta\mathbf{C})(\mathbf{W}_1^H + \mathbf{\Xi}_1^H) \right. \\ &\quad \cdot \left. ((\mathbf{W}_1 + \mathbf{\Xi}_1)(\mathbf{C} + \Delta\mathbf{C})(\mathbf{W}_1^H + \mathbf{\Xi}_1^H))^{-1}(\mathbf{W}_1 + \mathbf{\Xi}_1) \right\|_F^2 \approx \\ &= \left\| \mathbf{H}_1\mathbf{W}_1 - (\mathbf{C} + \Delta\mathbf{C})(\mathbf{W}_1^H + \mathbf{\Xi}_1^H) \cdot (\mathbf{W}_1\mathbf{C}\mathbf{W}_1^H + \right. \\ &\quad \left. \mathbf{W}_1\Delta\mathbf{C}\mathbf{W}_1^H + \mathbf{\Xi}_1\mathbf{C}\mathbf{W}_1^H + \mathbf{W}_1\mathbf{C}\mathbf{\Xi}_1^H)^{-1}(\mathbf{W}_1 + \mathbf{\Xi}_1) \right\|_F^2. \quad (46) \end{aligned}$$

Since \mathbf{W} is now the exact inverse of \mathbf{H} , it holds that $\mathbf{W}_1 \mathbf{C} \mathbf{W}_1^H = \mathbf{C}_{s_1}$. By neglecting higher than the first-order terms and by applying the first-order expansion of the matrix inverse inside the expression,

$$\begin{aligned} & \left\| \mathbf{H}_1 \mathbf{W}_1 - (\mathbf{C} + \Delta \mathbf{C})(\mathbf{W}_1^H + \mathbf{\Xi}_1^H)(\mathbf{I} + \mathbf{C}_{s_1}^{-1} \mathbf{\Xi}_1 \mathbf{C} \mathbf{W}_1^H + \right. \\ & \quad \left. + \mathbf{C}_{s_1}^{-1} \mathbf{W}_1 \Delta \mathbf{C} \mathbf{W}_1^H + \mathbf{C}_{s_1}^{-1} \mathbf{W}_1 \mathbf{C} \mathbf{\Xi}_1^H)^{-1} \mathbf{C}_{s_1}^{-1} (\mathbf{W}_1 + \mathbf{\Xi}_1) \right\|_F^2 \approx \\ & \left\| \mathbf{H}_1 \mathbf{W}_1 - (\mathbf{C} \mathbf{W}_1^H + \mathbf{C} \mathbf{\Xi}_1^H + \Delta \mathbf{C} \mathbf{W}_1^H)(\mathbf{I} - \mathbf{C}_{s_1}^{-1} \mathbf{\Xi}_1 \mathbf{C} \mathbf{W}_1^H - \right. \\ & \quad \left. - \mathbf{C}_{s_1}^{-1} \mathbf{W}_1 \Delta \mathbf{C} \mathbf{W}_1^H - \mathbf{C}_{s_1}^{-1} \mathbf{W}_1 \mathbf{C} \mathbf{\Xi}_1^H) \mathbf{C}_{s_1}^{-1} (\mathbf{W}_1 + \mathbf{\Xi}_1) \right\|_F^2. \quad (47) \end{aligned}$$

Since,

$$\begin{aligned} \mathbf{C} \mathbf{W}_1^H \mathbf{C}_{s_1}^{-1} &= \mathbf{H} \text{bdiag}(\mathbf{C}_{s_1}, \mathbf{C}_{s_2}) \mathbf{H}^H \mathbf{W}_1^H \mathbf{C}_{s_1}^{-1} \\ &= \mathbf{H}_1, \end{aligned} \quad (48)$$

the zero order term in (47) vanishes. By neglecting higher than the first-order terms, (29) follows. ■

ACKNOWLEDGMENTS

This work was supported by The Czech Science Foundation through Project No. 14-11898S and partly by California Community Foundation through Project No. DA-15-114599.

We thank BTL Medical Technologies CZ for providing us the three-channel ECG recording.

REFERENCES

- [1] H. L. Van Trees, *Optimum Array Processing: Part IV of Detection, Estimation, and Modulation Theory*, John Wiley & Sons, Inc., 2002.
- [2] P. Comon and C. Jutten, *Handbook of Blind Source Separation: Independent Component Analysis and Applications*, Academic Press, 2010.
- [3] J.-F. Cardoso, "Blind signal separation: statistical principles", *Proceedings of the IEEE*, vol. 90, n. 8, pp. 2009-2026, October 1998.
- [4] N. Q. K. Duong, E. Vincent, and R. Gribonval, Underdetermined reverberant audio source separation using a full-rank spatial covariance model, *IEEE Transactions on Audio, Speech, and Language Processing*, vol. 18, no. 7, pp. 1830-1840, Sept 2010.
- [5] H. Sawada, R. Mukai, S. Araki, and S. Makino, "A robust and precise method for solving the permutation problem of frequency-domain blind source separation," *IEEE Trans. Speech Audio Processing*, vol. 12, no. 5, pp. 530-538, 2004.
- [6] S. Ukai, T. Takatani, H. Saruwatari, K. Shikano, R. Mukai, H. Sawada, "Multistage SIMO-based Blind Source Separation Combining Frequency-Domain ICA and Time-Domain ICA, *IEICE Trans. Fundam.*, E88-A, no. 3, pp. 642-650, 2005.
- [7] K. Matsuoka and S. Nakashima, "Minimal distortion principle for blind source separation," *Proceedings of 3rd International Conference on Independent Component Analysis and Blind Source Separation (ICA '01)*, pp. 722-727, San Diego, Calif, USA, Dec. 2001.
- [8] S. Markovich, S. Gannot and I. Cohen, Multichannel Eigenspace Beamforming in a Reverberant Noisy Environment with Multiple Interfering Speech Signals," *IEEE Transactions on Audio, Speech and Language Processing*, vol. 17, no. 6, pp. 1071-1086, Aug. 2009.
- [9] S. Sanei and J. A. Chambers, *EEG Signal Processing*, Wiley, July 2007.
- [10] L. De Lathauwer, B. De Moor, J. Vandewalle, "Fetal Electrocardiogram Extraction by Blind Source Subspace Separation", *IEEE Transactions on Biomedical Engineering*, Special Topic Section on Advances in Statistical Signal Processing for Biomedicine, vol. 47, no. 5, pp. 567-572, May 2000.
- [11] A. Hyvärinen, J. Karhunen, and E. Oja, *Independent Component Analysis*, Wiley-Interscience, New York, 2001.
- [12] T. Kim, I. Lee; T.-W. Lee, "Independent Vector Analysis: Definition and Algorithms," *The Fortieth Asilomar Conference on Signals, Systems and Computers*, pp. 1393-1396, 2006.

- [13] M. Anderson, G. Fu, R. Phlypo, T. Adali, "Independent Vector Analysis: Identification Conditions and Performance Bounds," *IEEE Transactions on Signal Processing*, vol. 62, no. 17, pp. 4399–4410, 2014.
- [14] D. D. Lee and H. S. Seung, "Learning the parts of objects by non-negative matrix factorization," *Nature*, vol. 401, pp. 788–791, Oct. 1999.
- [15] A. Hyvärinen, "Fast and Robust Fixed-Point Algorithms for Independent Component Analysis," *IEEE Transactions on Neural Networks*, vol. 10, no. 3, pp. 626–634, 1999.
- [16] J.-F. Cardoso and A. Souloumiac, "Blind Beamforming from non-Gaussian Signals," *IEE Proc.-F*, vol. 140, no. 6, pp. 362–370, Dec. 1993.
- [17] S. A. Cruces-Alvarez, A. Cichocki, and S. Amari, "From Blind Signal Extraction to Blind Instantaneous Signal Separation: Criteria, Algorithms, and Stability," *IEEE Transactions on Neural Networks*, vol. 15, no. 4, July 2004.
- [18] D. Lahat, J.-F. Cardoso, and H. Messer, "Blind Separation of Multidimensional Components via Subspace Decomposition: Performance Analysis," *IEEE Transactions on Signal Processing*, vol. 62, no. 11, pp. 2894–2905, June 2014.
- [19] A. Hyvärinen and U. Köster, "FastISA: A fast fixed-point algorithm for independent subspace analysis," *In Proc. European Symposium on Artificial Neural Networks*, Bruges, Belgium, 2006.
- [20] J. Cardoso, "Multidimensional independent component analysis," in *Proceedings of the 1998 IEEE International Conference on Acoustics, Speech and Signal Processing*, vol. 4, pp. 1941–1944, 12–15 May 1998.
- [21] D. Lahat, J.-F. Cardoso, and H. Messer, "Second-order multidimensional ICA: performance analysis," *IEEE Transactions on Signal Processing*, vol. 60, no. 9, pp. 4598–4610, Sept. 2012.
- [22] Z. Koldovský and P. Tichavský, "Time-domain blind separation of audio sources on the basis of a complete ICA decomposition of an observation space," *IEEE Trans. on Speech, Audio and Language Processing*, vol. 19, no. 2, pp. 406–416, Feb. 2011.
- [23] J. Capon, "High-resolution frequency-wavenumber spectrum analysis," *Proc. of IEEE*, vol. 57, no. 8, pp. 1408–1418, Aug. 1969.
- [24] P. Tichavský and Z. Koldovský, "Optimal Pairing of Signal Components Separated by Blind Techniques," *IEEE Signal Processing Letters*, vol. 11, no. 2, pp. 119–122, 2004.
- [25] T. Kim, H. T. Attias, S.-Y. Lee, T.-W. Lee, "Blind Source Separation Exploiting Higher-Order Frequency Dependencies," *IEEE Transactions on Audio, Speech, and Language Processing*, vol. 15, no. 1, Jan. 2007.
- [26] J. F. Cardoso, M. Le Jeune, J. Delabrouille, M. Betoule and G. Patanchon, "Component Separation With Flexible Models Application to Multichannel Astrophysical Observations," *IEEE Journal of Selected Topics in Signal Processing*, vol. 2, no. 5, pp. 735–746, Oct. 2008.
- [27] The Planck collaboration, "Planck 2013 results. XII. Diffuse component separation," *Astronomy and Astrophysics*, vol. 571, A12, Nov. 2014.
- [28] J.-F. Cardoso, "On the performance of orthogonal source separation algorithms," *Proc. EUSIPCO*, pp. 776–779, Edinburgh, September 1994.
- [29] K. Matsuoka, "Elimination of filtering indeterminacy in blind source separation," *Neurocomputing*, vol. 71, pp. 2113–2126, 2008.
- [30] P. Tichavský, Z. Koldovský, and E. Oja, "Performance Analysis of the FastICA Algorithm and Cramér-Rao Bounds for Linear Independent Component Analysis," *IEEE Trans. on Signal Processing*, Vol. 54, No. 4, April 2006.
- [31] S. Makino, Te-Won Lee, and H. Sawada, *Blind Speech Separation*, Springer, Sept. 2007.
- [32] Parra, L., and Spence, C.: "Convolutional Blind Separation of Non-Stationary Sources," *IEEE Trans. on Speech and Audio Processing*, Vol. 8, No. 3, pp. 320–327, May 2000.
- [33] F. Nesta and M. Matassoni, "Blind source extraction for robust speech recognition in multisource noisy environments," *Journal Computer Speech and Language*, vol. 27, no. 3, pp. 730–725, May 2013.
- [34] J. Benesty, J. Chen, and E. Habets, *Speech Enhancement in the STFT Domain*, Springer Briefs in Electrical and Computer Engineering, 2011.
- [35] F. Abrard, Y. Deville, "A time-frequency blind signal separation method applicable to underdetermined mixtures of dependent sources," *Signal Processing*, vol. 85, issue 7, pp. 1389–1403, July 2005.
- [36] T.-W. Lee, M. S. Lewicki, M. Girolami, T. J. Sejnowski, "Blind Source Separation of More Sources Than Mixtures Using Overcomplete Representations," *IEEE Signal Processing Letters*, vol. 6, no. 4, 1999.
- [37] L. Griffiths and C. Jim, "An alternative approach to linearly constrained adaptive beamforming," *IEEE Trans. Antennas Propag.*, vol. 30, no. 1, pp. 27–34, Jan. 1982.
- [38] J. Even, C. Ishi, H. Saruwatari, and N. Hagita, "Close speaker cancellation for suppression of non-stationary background noise

- for hands-free speech interface,” *Proc. of the 11th Annual Conference of the International Speech Communication Association (Interspeech 2010)*, pp. 977-980, Makuhari, Chiba, Japan, September 26-30, 2010.
- [39] O. Hoshuyama, A. Sugiyama, A. Hirano, “A robust adaptive beamformer for microphone arrays with a blocking matrix using constrained adaptive filters,” *IEEE Transactions on Signal Processing*, vol. 47, no. 10, pp. 2677–2684, Oct. 1999.
- [40] Y. Takahashi, T. Takatani, K. Osako, H. Saruwatari, K. Shikano, “Blind Spatial Subtraction Array for Speech Enhancement in Noisy Environment,” *IEEE Transactions on Audio, Speech, and Language Processing*, vol. 17, no. 4, pp. 650–664, May 2009.
- [41] Vincent, E., Gribonval, R., and C. Févotte, “Performance Measurement in Blind Audio Source Separation,” *IEEE Trans. on Speech and Audio Processing*, Vol 14, No. 4, pp. 1462–1469, July 2006.
- [42] S. Gannot, D. Burshtein, and E. Weinstein, “Signal enhancement using beamforming and nonstationarity with applications to speech,” *IEEE Trans. on Signal Processing*, vol. 49, no. 8, pp. 1614–1626, Aug. 2001.
- [43] S. Gannot and I. Cohen, “Speech Enhancement Based on the General Transfer Function GSC and Postfiltering,” *IEEE Trans. on Speech and Audio Processing*, vol. 12, No. 6, pp. 561–571, Nov. 2004.
- [44] Z. Koldovský, J. Málek, and S. Gannot, “Spatial Source Subtraction Based on Incomplete Measurements of Relative Transfer Function,” *IEEE/ACM Trans. on Speech, Audio and Language Processing*, vol. 23, no. 8, pp. 1335–1347, Aug. 2015.
- [45] Z. Koldovský, F. Nesta, P. Tichavský, and N. Ono, “Frequency-Domain Blind Speech Separation Using Incomplete De-Mixing Transform,” *The 24th European Signal Processing Conference (EUSIPCO 2016)*, pp. 1663–1667, Budapest, Hungary, Sept. 2016.
- [46] R. Tibshirani, “Regression shrinkage and selection via the lasso,” *J. Royal. Statist. Soc. B.*, vol. 58, pp. 267–288, 1996.
- [47] J. Janský, Z. Koldovský and N. Ono, “A Computationally Cheaper Method for Blind Speech Separation Based On AuxIVA and Incomplete Demixing Transform,” *The 15th International Workshop on Acoustic Signal Enhancement (IWAENC)*, Xian, China, Sept. 2016.



Zbyněk Koldovský (M’04-SM’15) was born in Jablonec nad Nisou, Czech Republic, in 1979. He received the M.S. degree and Ph.D. degree in mathematical modeling from Faculty of Nuclear Sciences and Physical Engineering at the Czech Technical University in Prague in 2002 and 2006, respectively. He was also with the Institute of Information Theory and Automation of the Academy of Sciences of the Czech Republic from 2002 to 2016.

Currently, he is an associate professor at the Institute of Information Technology and Electronics, Technical University of Liberec, and the leader of Acoustic Signal Analysis and Processing (A.S.A.P.) Group. He is the Vice-dean for Science, Research and Doctoral Studies at the Faculty of Mechatronics, Informatics and Interdisciplinary Studies. His main research interests are focused on audio signal processing, blind source separation, independent component analysis, and sparse representations.

Zbyněk Koldovský has served as a general co-chair of the 12th Conference on Latent Variable Analysis and Signal Separation (LVA/ICA 2015) in Liberec, Czech Republic.



Francesco Nesta received the Laurea degree in computer engineering from Politecnico di Bari, Bari, Italy, in September 2005 and the Ph.D. degree in information and communication technology from University of Trento, Trento, Italy, in April 2010, with research on blind source separation and localization in adverse environments.

He has been conducting his research at Bruno Kessler Foundation IRST, Povo di Trento, from 2006 to 2012. He was a Visiting Researcher from September 2008 to April 2009 with the Center for Signal and Image Processing Department, Georgia Institute of Technology, Atlanta. His major interests include statistical signal processing, blind source separation, speech enhancement, adaptive filtering, acoustic echo cancellation, semi-blind source separation and multiple acoustic source localization. He is currently working at Conexant System, Irvine (CA, USA) on the development of audio enhancement algorithms for far-field applications.

Dr. Nesta serves as a reviewer for several journals such as the *IEEE TRANSACTION ON AUDIO, SPEECH, AND LANGUAGE PROCESSING*, *Elsevier Signal Processing Journal*, *Elsevier Computer Speech and Language*, and in several conferences and workshops in the field of acoustic signal processing. He has served as Co-Chair in the third community-based Signal Separation Evaluation Campaign (SiSEC 2011) and as organizer of the 2nd CHIME challenge.